

Insights into malaria susceptibility using genome-wide data on 17,000 individuals from Africa, Asia and Oceania

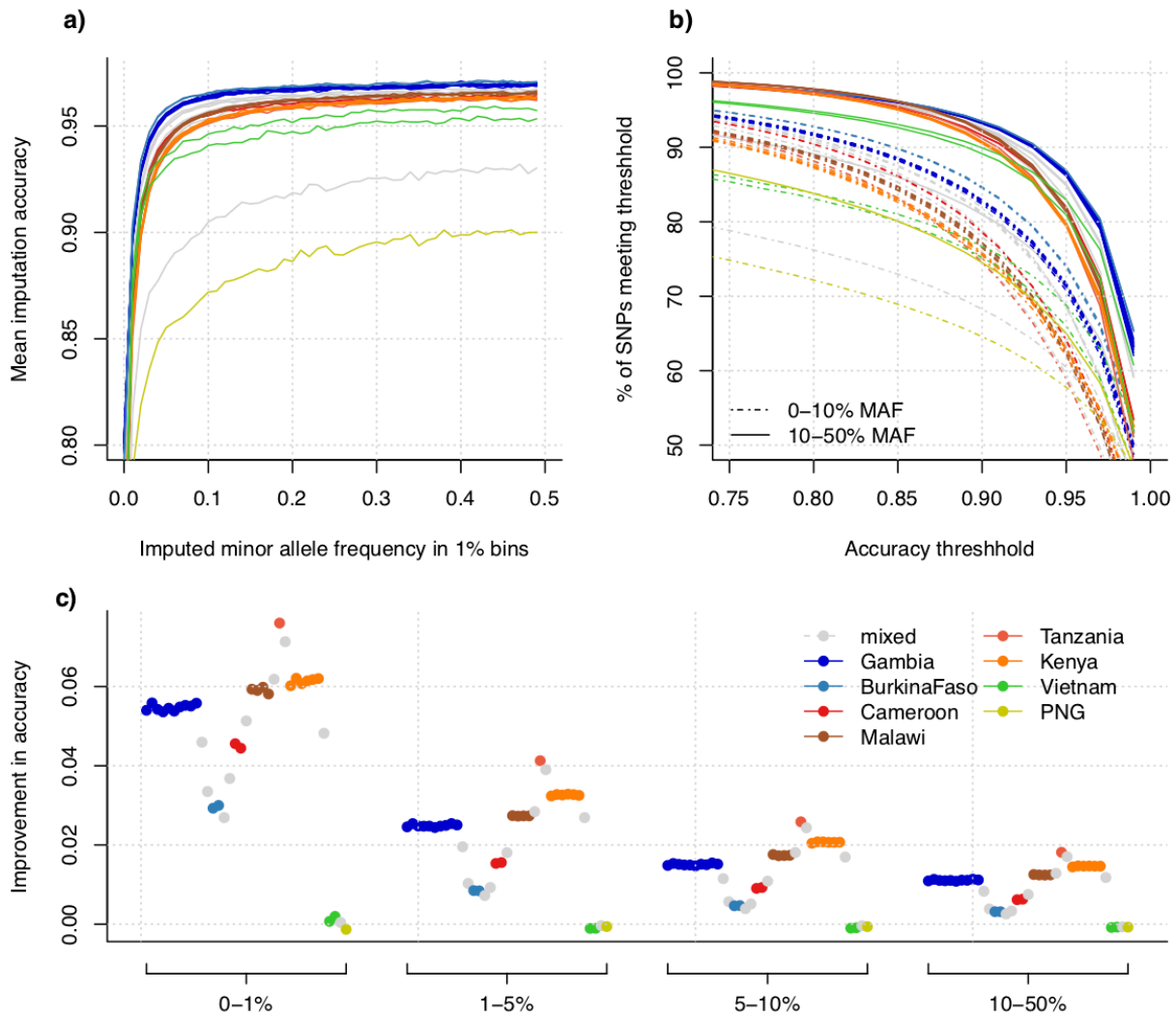
Malaria Genomic Epidemiology Network

Supplementary information

Contents:

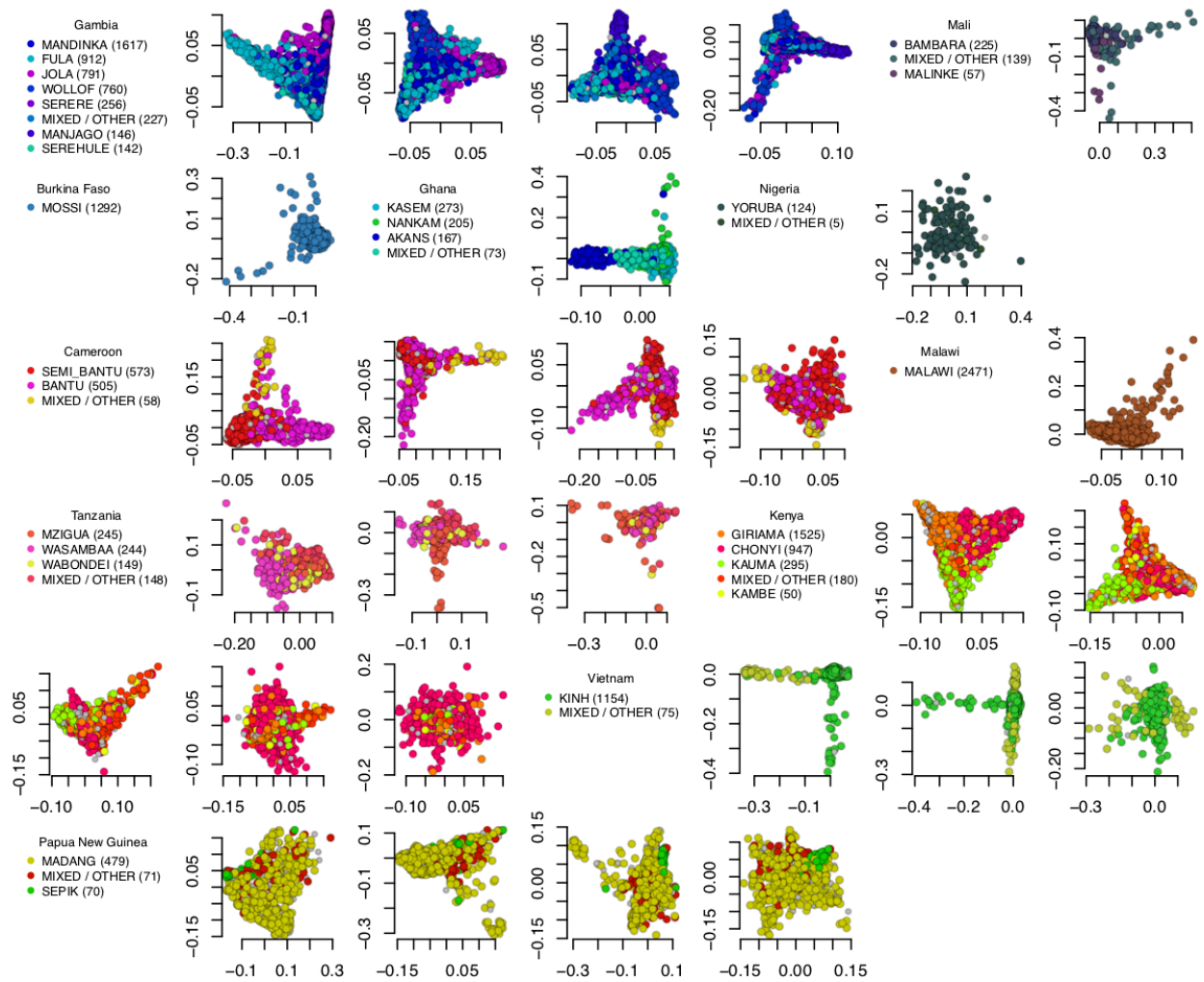
<i>Supplementary Figure 1 - Detail of imputation accuracy.</i>	2
<i>Supplementary Figure 2 - Principal components (PCs) across all study samples.</i>	3
<i>Supplementary Figure 3 - Manhattan plot for case-control and subphenotype tests.</i>	4
<i>Supplementary Figure 4 - Analysis of the heritability of SM across African study populations</i>	5
<i>Supplementary Figure 5 - Discovery and replication effect sizes for variants in Figure 2c (part 1)</i>	7
<i>Supplementary Figure 6 - Discovery and replication effect sizes for variants in Figure 2c (part 2)</i>	9
<i>Supplementary Figure 7 - Discovery and replication effect sizes for variants in HLA and AP2B1</i>	10
<i>Supplementary Figure 8 - joint derived allele frequency distribution of African and European populations</i>	11
<i>Supplementary Figure 9 - Empirical model of allele frequencies across African populations</i>	12
<i>Supplementary Figure 10 - Illustration of the empirical model of allele frequencies across African populations at different frequencies</i>	13
<i>Supplementary Figure 11 - Evidence for within-Africa differentiation at variants across the genome</i>	14
<i>Supplementary Figure 12 - Mendelian randomization analysis with 36 haematopoietic traits</i>	15
<i>Supplementary Figure 13 - Comparison of reference panel and study frequencies at typed SNPs</i>	16
<i>Supplementary Figure 14 - Average X and Y channel intensity values per sample in each population, and intensity exclusions.</i>	17
<i>Supplementary Figure 15 - average missing call and heterozygosity rates per sample, and sample exclusions.</i>	18
<i>Supplementary Figure 16 - Average X+Y channel intensities across sex chromosomes, and gender assignment.</i>	19
<i>Supplementary Figure 17 - cumulative distribution of per-sample missingness.</i>	20
<i>Supplementary Figure 18 - Detail of QC: manhattan plots.</i>	21
<i>Supplementary Figure 19 - Array intensities and genotyping near the end of chromosome 19</i>	22
<i>Supplementary Figure 20 - Illustration of replication effect size model.</i>	23
<i>Supplementary Table 1 - Detail of partner studies and ethics approval.</i>	24
<i>Supplementary Table 2 - Previous publications</i>	25
<i>Supplementary Table 3 - Detail of Sample QC</i>	26
<i>Supplementary Table 4 - Detail of SNP QC</i>	27
<i>Supplementary Table 5 - Detail of models included in BF_{avg}</i>	28
<i>Supplementary Note 1 - Investigation of the HBA1-HBA2 region</i>	29
<i>Supplementary Note 2 - Investigation of the basigin region</i>	30
<i>Supplementary Note 3 - Investigation of association in G6PD and CD40LG</i>	31
<i>Supplementary Note 4 - Analysis of functional annotations</i>	32
<i>Supplementary Note 5 - Bayesian analysis of replication</i>	33
<i>Supplementary Note 6 - Genome-wide implementation of multinomial logistic regression</i>	34
<i>Supplementary Note 7 - Multidimensional inverse variance-weighted meta-analysis</i>	35
<i>Supplementary Note 8 - Analysis of population differentiation</i>	36

Supplementary Figures



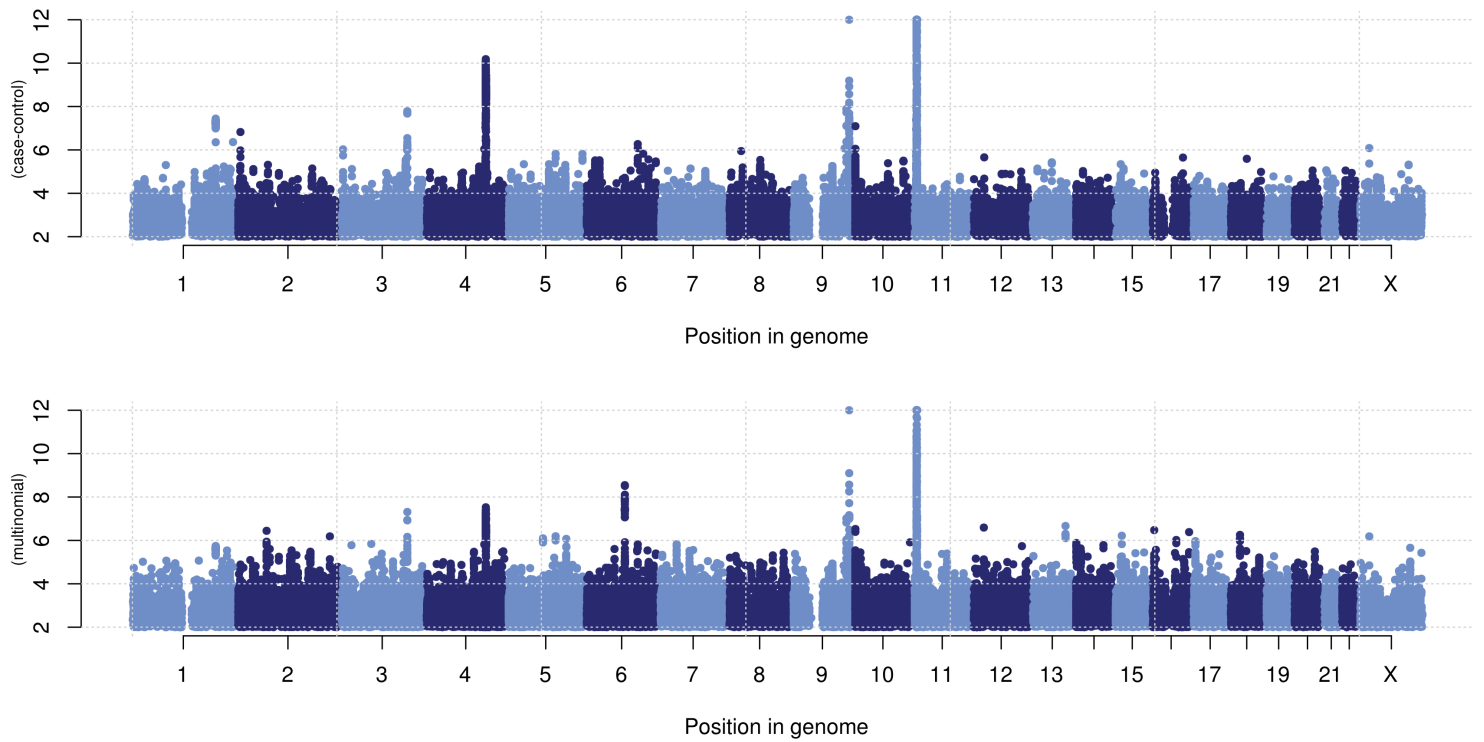
Supplementary Figure 1 - Detail of imputation accuracy.

a) Per-variant imputation accuracy (computed as the mean squared correlation between directly typed and reimputed genotypes, evaluated at Omni 2.5M SNPs included in the imputation) against minor allele frequency for all samples in our study. Imputation was performed in sets of 500 samples; each line represents a single sample set. Lines are coloured by population (if all samples in the set were from a single population) or grey if samples from a mixture of populations was included, according to the legend in panel c). b) The proportion of variants at or above a given imputation accuracy, for accuracies in the range 0.75-1, as computed by masking and re-imputing typed SNPs. For example, in African sample sets over 90% of common variants were reimputed with at least 90% accuracy. c) Improvement in per-variant imputation accuracy between the combined panel and the 1000 Genomes reference panel. Improvement is computed as the mean difference in accuracy for variants in the given minor allele frequency bin (x axis); each point represents a single imputation run of 500 samples.



Supplementary Figure 2 - Principal components (PCs) across all study samples.

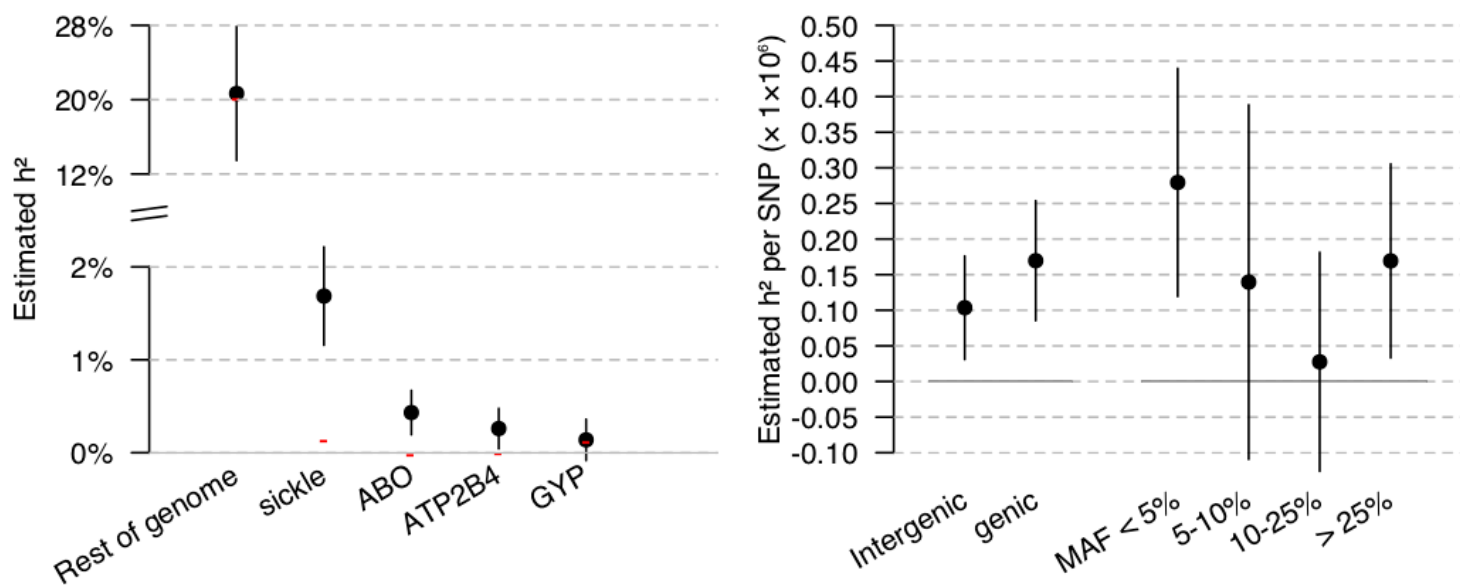
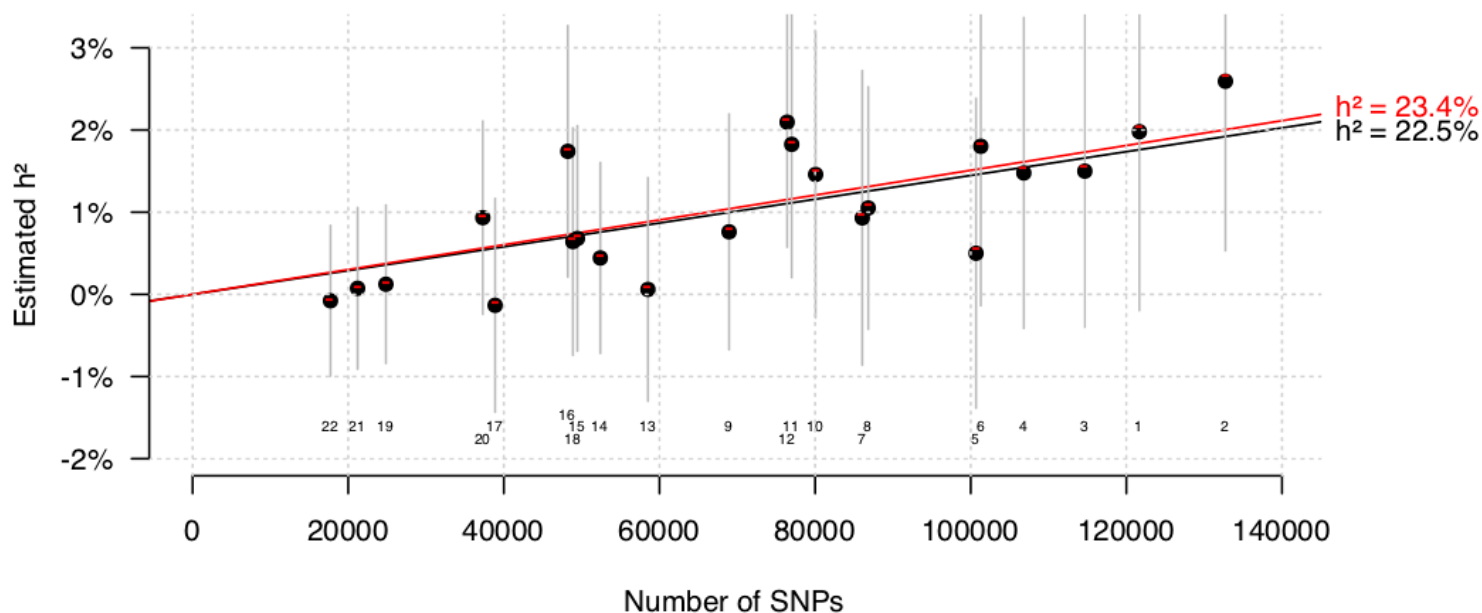
Selected PCs computed in each population using the phased genotype calls. For each study population, a summary of the ethnic makeup of the study samples is given, followed by a plot of the first PC (x axis) versus the second PC (y axis). For populations displaying more structure we also plot the 2nd versus 3rd PC, the 3rd versus 4th PC, etc. Colours are chosen to distinguish ethnic groups, with the largest ethnic group being set to the population colour, as shown in **Figure 1**, and other ethnic groups given a spread of hues around the population colour. In each population we plot samples in random order to avoid visual overrepresentation of specific ethnicities.



Supplementary Figure 3 - Manhattan plot for case-control and subphenotype tests.

a) $-\log_{10}$ P-value for an additive model of association of the genotype on SM status, versus controls, for each SNP included in our analysis. Effect size estimates and standard errors are computed in each study population using logistic regression (as implemented in SNPTTEST) including 5 principal components of population structure. Results are then meta-analysed across populations using fixed-effect meta-analysis.

b) $-\log_{10}$ P-value for an additive model of association of the genotype with CM, SMA, or OTHER phenotypes, relative to controls. Results are computed using multinomial logistic regression in each study population including 5 principal components. Results are then meta-analysed across populations using fixed-effect meta-analysis.

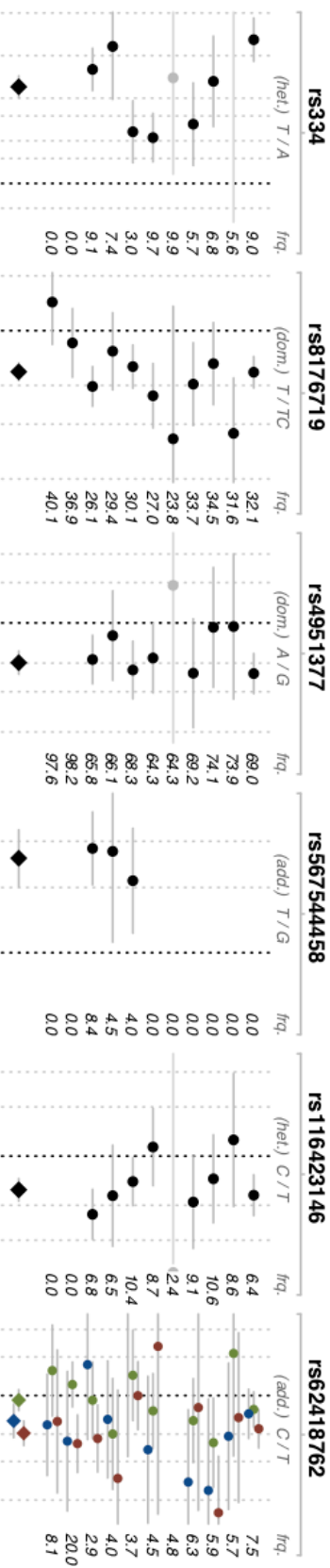


Supplementary Figure 4 - Analysis of the heritability of SM across African study populations

Results are based on a joint analysis of 13,038 individuals, selected to have <5% pairwise relatedness within each African study site, using the phased dataset of 1,550,514 SNPs. We included 20 PCs computed across these individuals, as well as an indicator of study site as fixed effects to control for population structure. Results are estimated using PCGC. a) Estimated heritability attributed to each chromosome when including all chromosomes jointly in the model (black points, with grey bars indicating 95% confidence intervals; small text indicates chromosome number) and when estimating for each chromosome separately (red horizontal lines). Sloping lines indicate the overall estimated heritability for each model. A small degree of inflation is seen when using separate estimates, indicating there may be some residual confounding by population structure. b) Estimates for heritability across previously identified regions of association and to the rest of the genome, when fit jointly (black points and line segments). Red bars indicate estimates after including the dosage of the lead SNP in each of the four association regions as a covariate. c) Residual estimates for heritability partitioned into genic and intergenic regions (left two points), and into minor allele frequency bins. Estimates are made excluding the four association regions in b) and are conditional on the protective dosage at these variants. Additional details can be found in **Supplementary Data 2**.

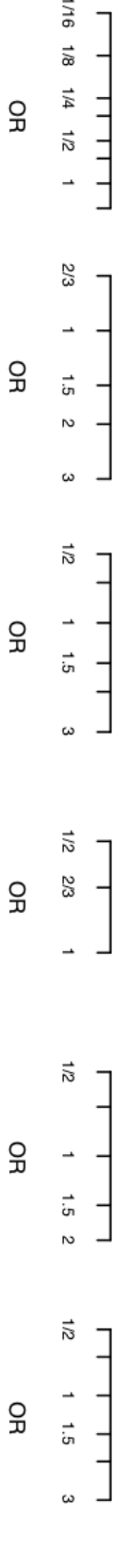
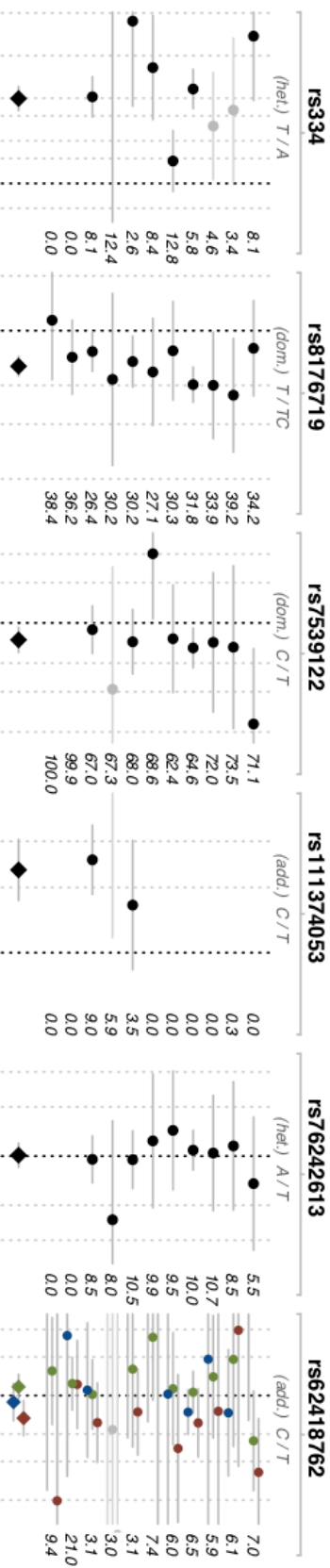
Discovery

	CONTROL	SM	SMA	CM+SMA	OTHER
Gambia	2605	780	456	134	1197
Mali	183	61	81	51	70
BurkinaFaso	596	94	28	18	593
Ghana	320	31	41	5	322
Nigeria	22	28	1	0	80
Cameroun	685	32	66	8	486
Malawi	1317	642	65	109	366
Tanzania	403	31	178	25	182
Kenya	1615	690	174	189	628
Vietnam	546	154	23	4	537
PNG	374	49	115	7	228
Meta-analysis	8666	2592	1228	550	4689



Replication

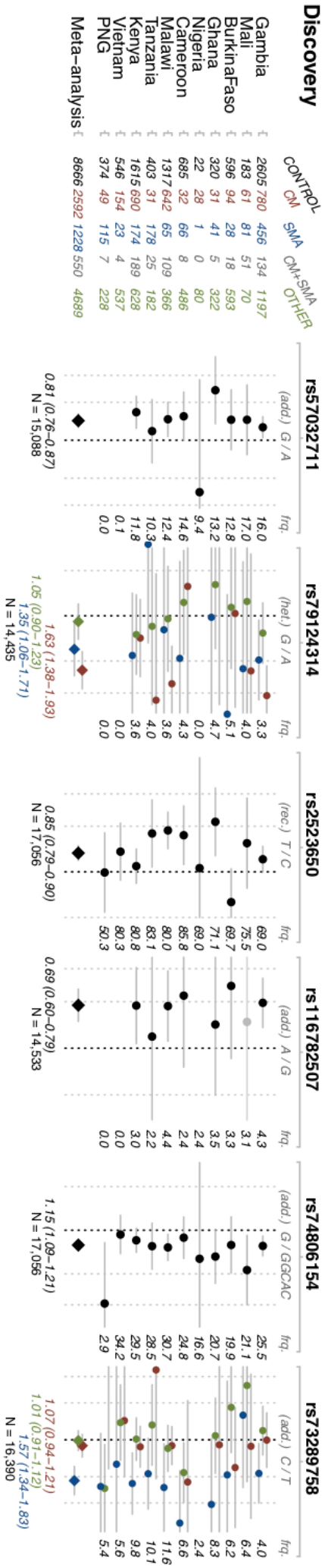
	CONTROL	SM	SMA	CM+SMA	OTHER
Gambia	266	79	39	13	124
Mali	190	27	106	30	61
BurkinaFaso	194	23	13	3	198
Ghana	2016	252	784	89	1010
Nigeria	194	55	8	0	238
Cameroun	184	11	34	3	186
Malawi	2154	297	75	64	128
Tanzania	101	4	25	5	37
Kenya	2508	313	134	86	585
Vietnam	1996	82	8	4	178
PNG	156	3	17	2	174
Meta-analysis	9959	1126	1243	299	2919



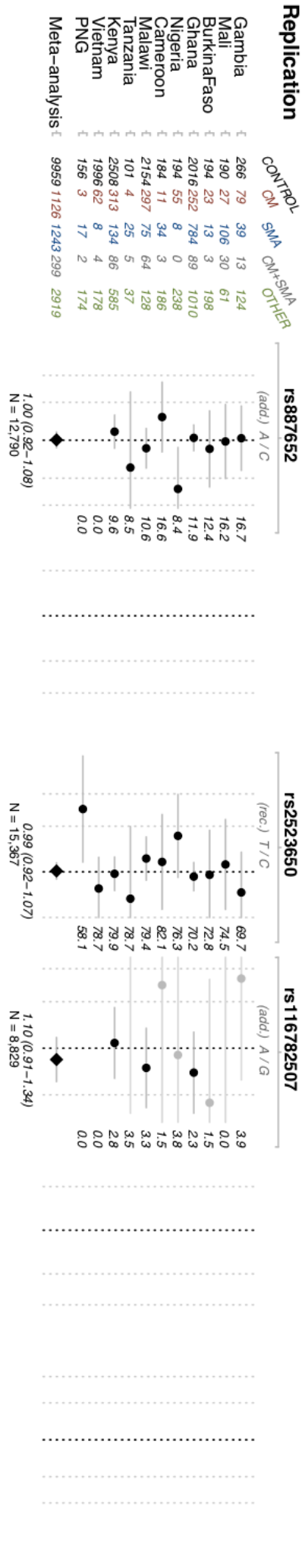
Supplementary Figure 5 - Discovery and replication effect sizes for variants in Figure 2c (part 1)

Figure shows sample counts, effect size estimates and confidence intervals for association tests with the top six variants in **Figure 2c**. For each variant, the top panel shows discovery analysis (using imputed genotypes) and the bottom panel shows replication analysis using directly-typed genotypes at the best Sequenom tag, as defined in Methods. Within each panel, rows show the population label and counts of controls and of cases reported as CM, SMA, CM and SMA, or OTHER severe malaria phenotypes, with the bottom row indicating the total sample count available for meta-analysis. For each variant, data is presented for the mode of inheritance and choice of case/control or subphenotype effects forming the best posterior model identified by our discovery analysis (as shown in **Figure 2c**), with these choices indicated at the top of the plot along with the reference and non-reference alleles. For each variant, the plot depicts the estimated effect size (OR, points) and 95% confidence interval (line segments) for the non-reference allele on severe malaria (black points) or on severe malaria subphenotypes (red points, CM; blue points, SMA; green points, OTHER SM). Points corresponding to estimates based on fewer than 25 observations of the minor allele (or minor predictor for non-additive model estimates) are depicted in grey; these were not included in meta-analysis computation (**Methods**). Text under each plot indicates the odds ratio and confidence interval computed using fixed-effect meta-analysis across populations, and the total sample size contributing to the meta-analysis. To the right, the frequency of the non-reference allele estimated using control samples in each population is indicated. Source data are provided as a Source Data file.

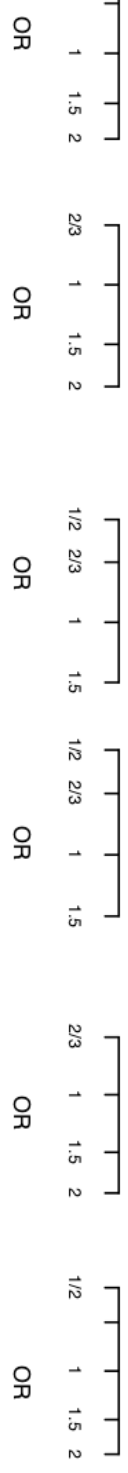
Discovery



Replication



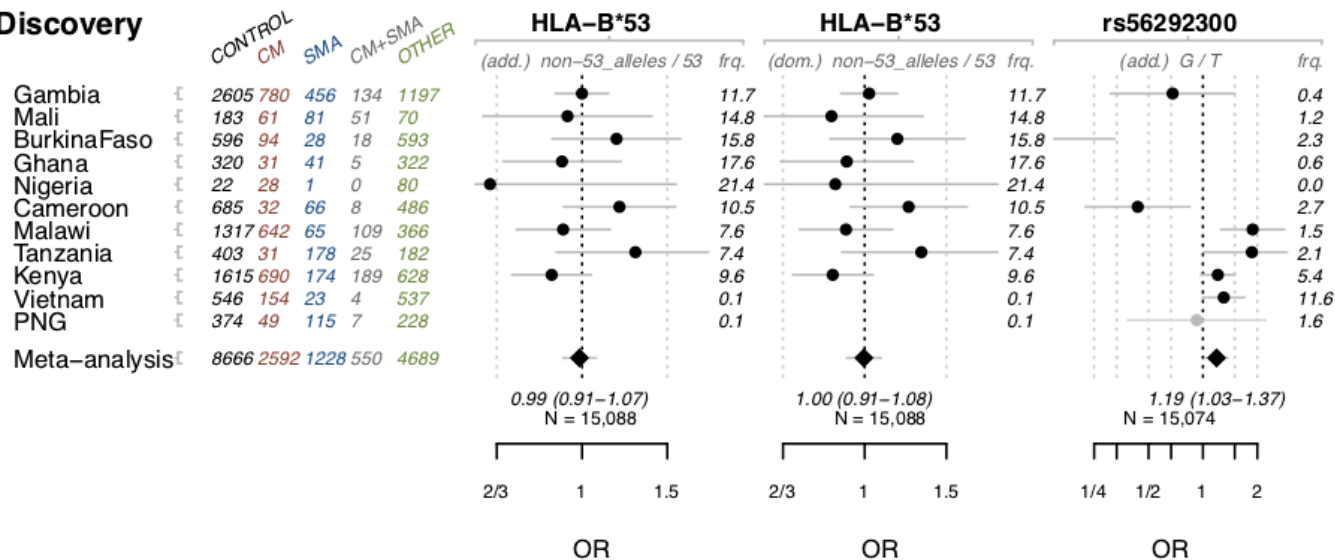
	CONTROL	CM	SMA	CM+SMA	OTHER
Gambia	266	79	39	13	124
Mali	190	27	106	30	61
BurkinaFaso	194	23	13	3	198
Ghana	2016	252	784	89	1010
Nigeria	194	55	8	0	238
Cameroon	184	11	34	3	186
Malawi	2154	297	75	64	128
Tanzania	101	4	25	5	37
Kenya	2508	313	134	86	585
Vietnam	1996	62	8	4	178
PNG	156	3	17	2	174
Meta-analysis	9959	1126	1243	299	2919



Supplementary Figure 6 - Discovery and replication effect sizes for variants in Figure 2c (part 2)

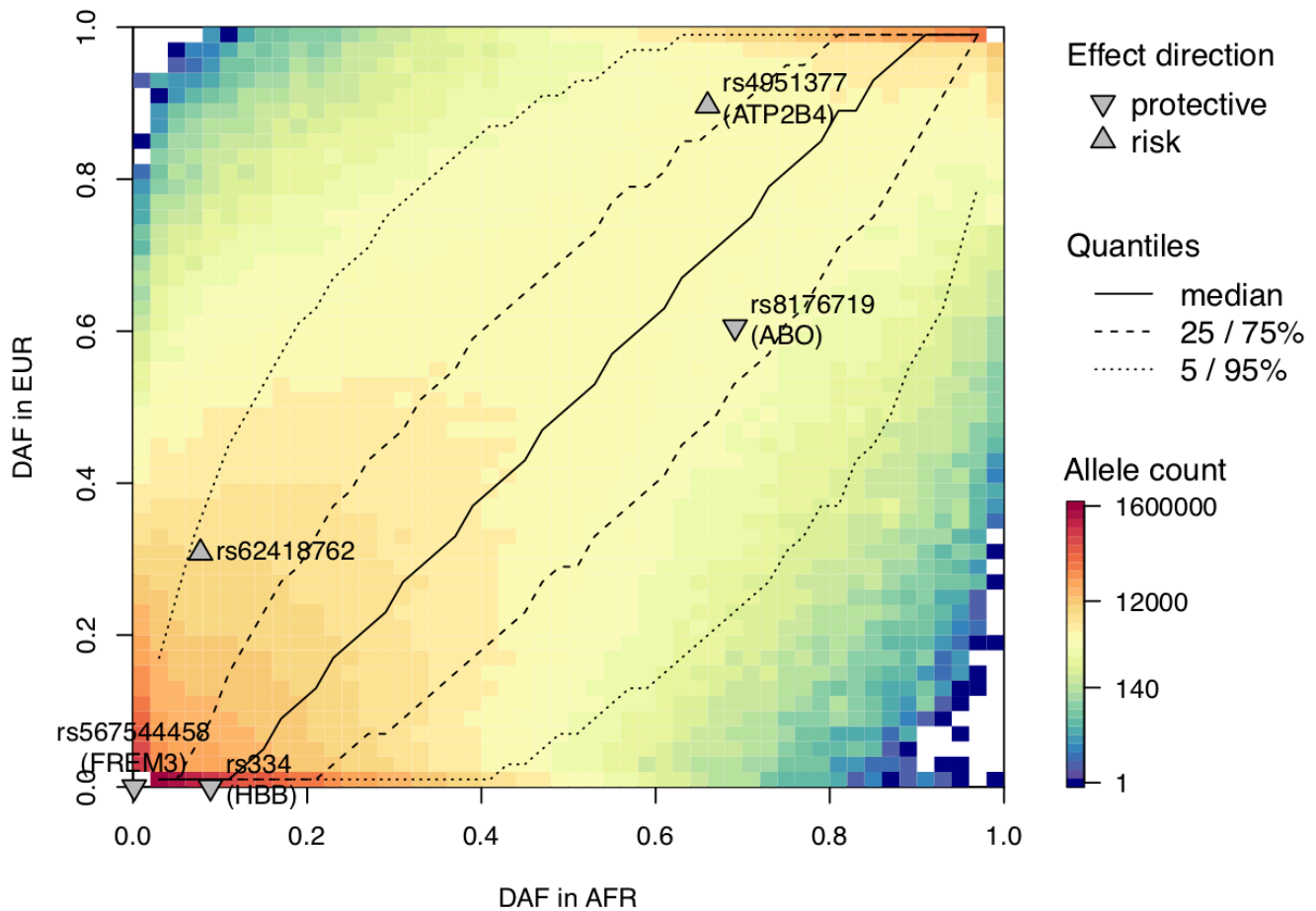
Figure shows sample counts, effect size estimates and confidence intervals for association tests with the bottom six variants in **Figure 2c**. See **Supplementary Figure 5** legend for details. A blank lower panel indicates a discovery variant for which no valid Sequenom tag was available (**Methods** and **Supplementary Data 1**). Source data are provided as a Source Data file.

Discovery



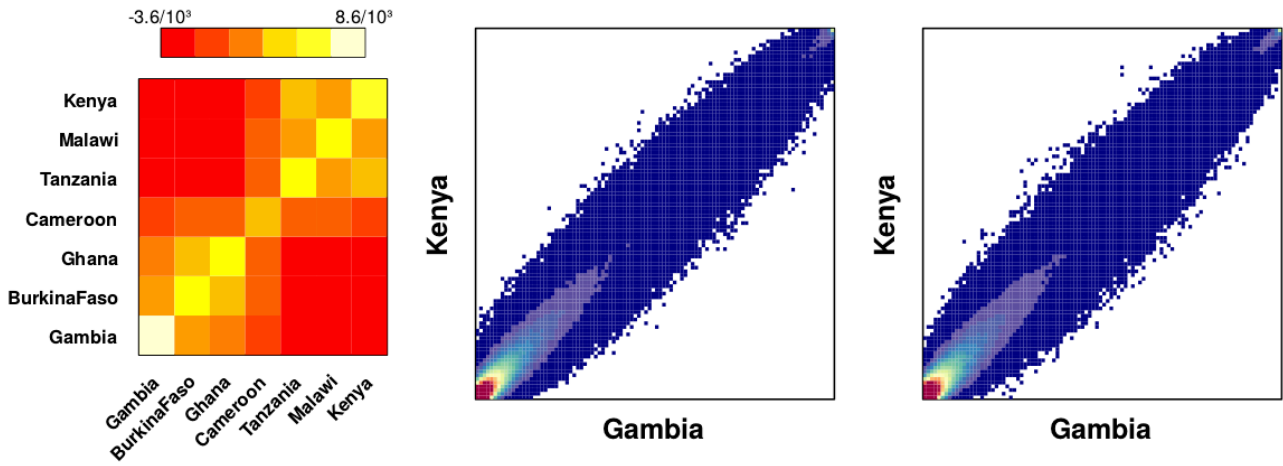
Supplementary Figure 7 - Discovery and replication effect sizes for variants in HLA and *AP2B1*

Figure shows discovery effect size estimates and confidence intervals for HLA-B*53 under additive and dominance model of association, and for rs56292300. See Supplementary **Figure 5** legend for details. Source data are provided as a Source Data file.



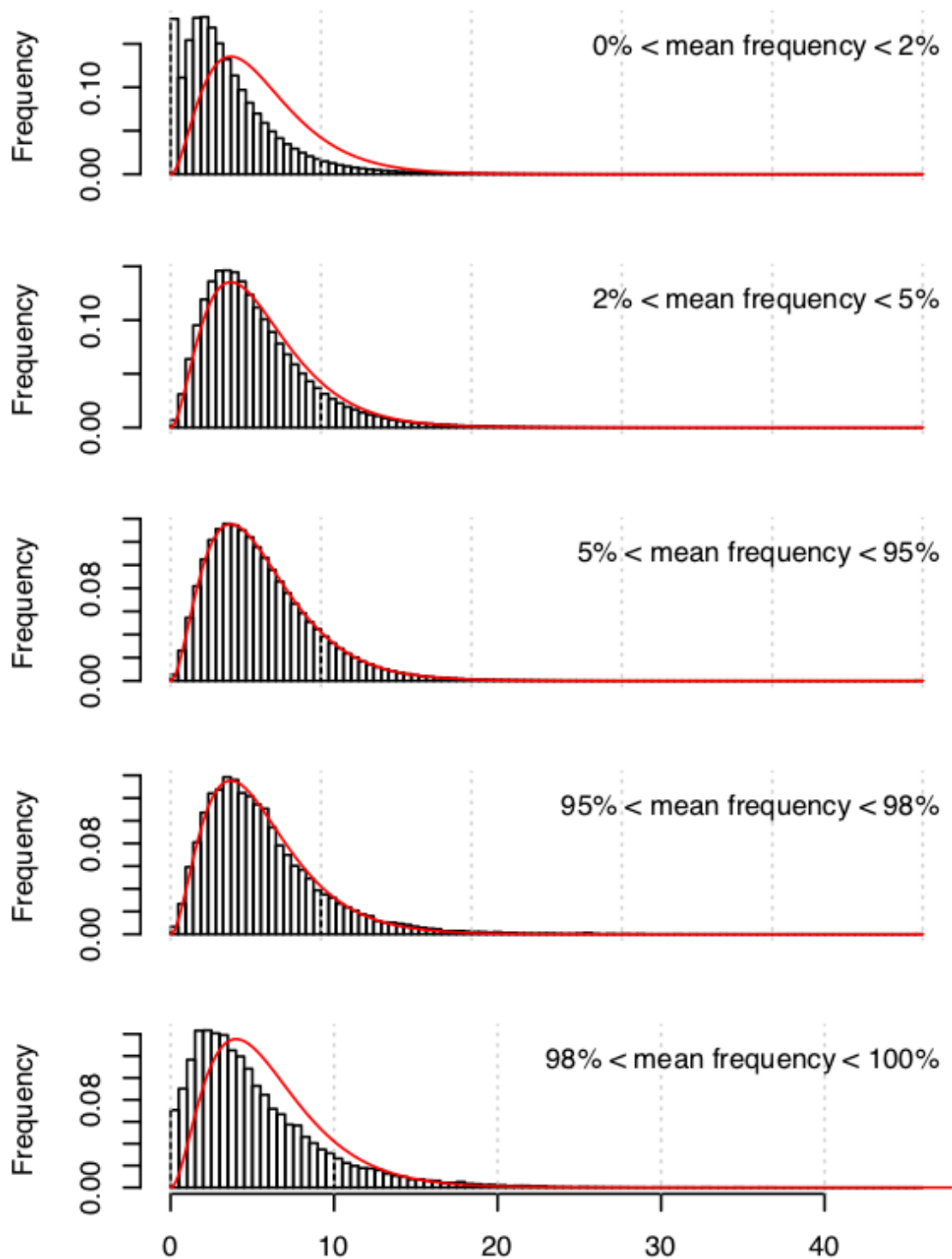
Supplementary Figure 8 - joint derived allele frequency distribution of African and European populations

Plot shows the empirical distribution of allele counts for derived (i.e. non-ancestral) alleles in African (x axis) and European (y axis) reference panel samples. Counts are aggregated into 1% frequency bins for visualization; colours indicate the number of alleles in each bin according to the scale on the right. Only variants not masked by the 1000 Genomes 'strict' mask, and having an ancestral allele assignment in the 1000 Genomes ancestral allele sequence are included. Black lines indicate the empirical median, 25%, and 5% quantiles of the distribution in Europe conditional on the African allele frequency (i.e. in each vertical 'slice' through the plot). Triangles indicate the position of the five replicating associations on the distribution, with 'up' arrows indicating that the risk allele is derived, and 'down' arrows indicating that the protective allele is derived. For each SNP, $rank_{EUR}$ can be computed as the tail of the vertical slice above (for protective derived alleles) or below (for risk derived alleles) the variant, in the direction of the triangle. We include half of the count of the bin containing the SNP so that both tails sum to one.



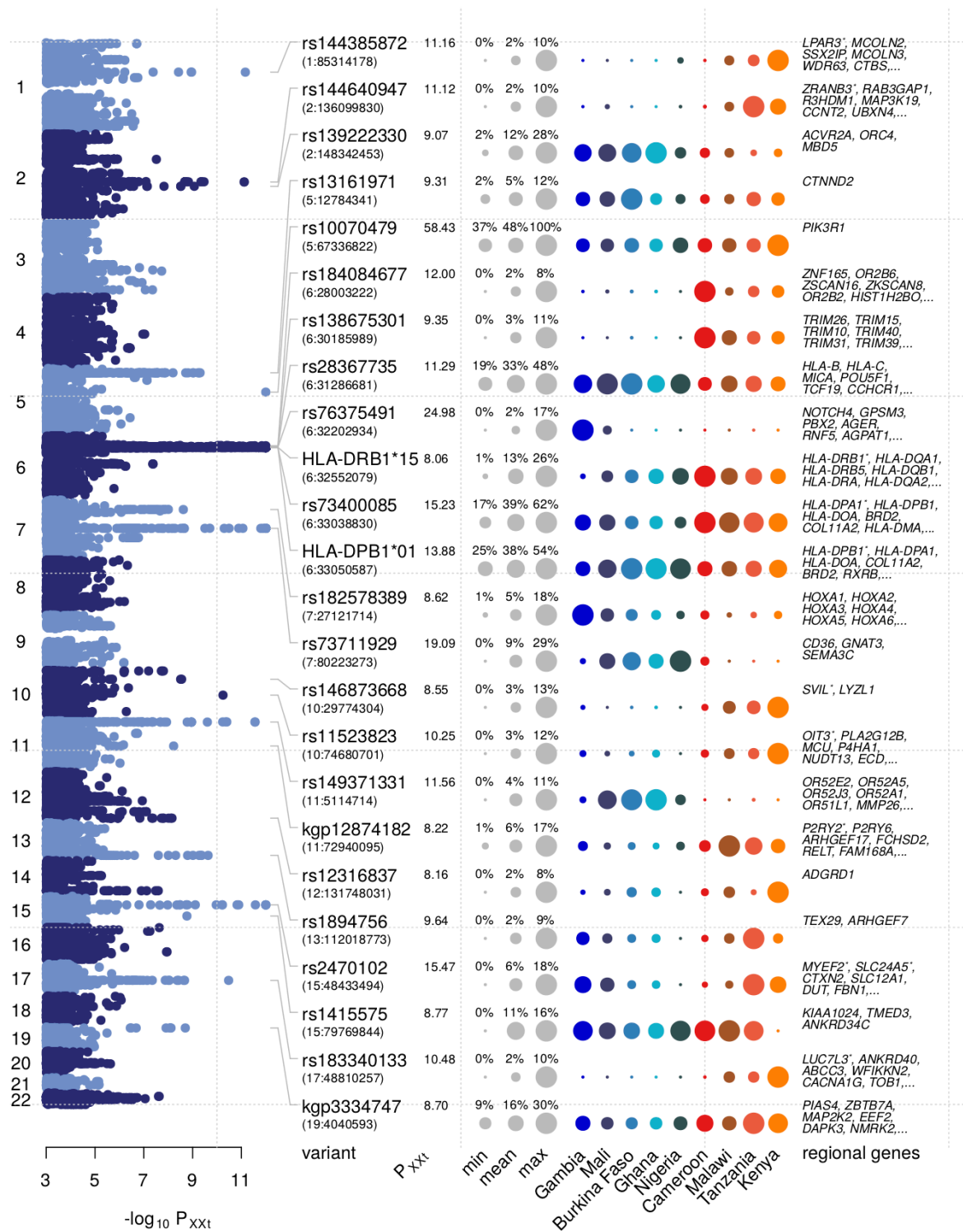
Supplementary Figure 9 - Empirical model of allele frequencies across African populations

Visualisation of an empirical model of allele frequencies estimated across the seven African study sites with at least 500 samples. Left: covariance matrix of scaled allele frequencies estimated at 100,000 SNPs, randomly chosen from among those have mean frequency in the range 2-98%. Covariance is computed from allele frequencies after subtracting the mean frequency (f_0) and dividing by the expected standard deviation $\sqrt{f_0(1-f_0)}$. b) the empirical joint distribution of allele frequencies in Kenya and The Gambia. c) illustration of the modelled distribution of allele frequencies, for 1,000,000 SNPs simulated from the model in panel a) based on mean frequency sampled from the empirical mean frequency distribution in Kenya and The Gambia. Given the root frequency f_0 , we simulated a scaled frequency vector v by sampling based on the estimated covariance matrix. We then plot the frequencies computed as $f_0 + v\sqrt{f_0(1-f_0)}$ in Gambia and Kenya.



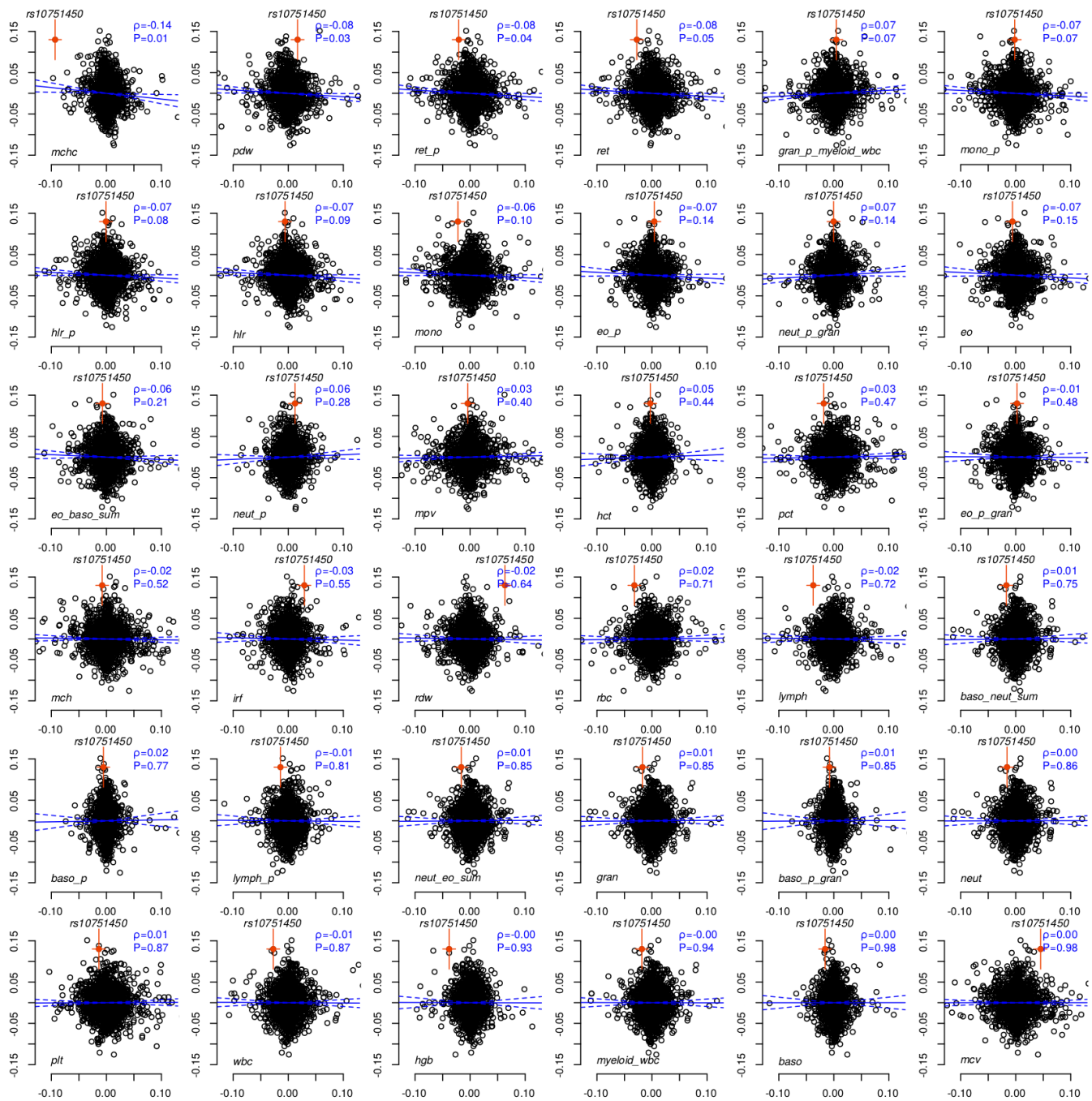
Supplementary Figure 10 - Illustration of the empirical model of allele frequencies across African populations at different frequencies

Bars show the empirical distribution of the $X'X$ statistic for all SNPs in the frequency bins indicated by the text. Red lines show the density of the χ^2 distribution used to compute $P_{X'X}$. The test reflects a 6-degree-of-freedom χ^2 distribution; we remove one population (Cameroon) from the test to account for subtracting the mean frequency. The theoretical distribution matches the true distribution closely, except for rarer variants where the theoretical distribution appears conservative.



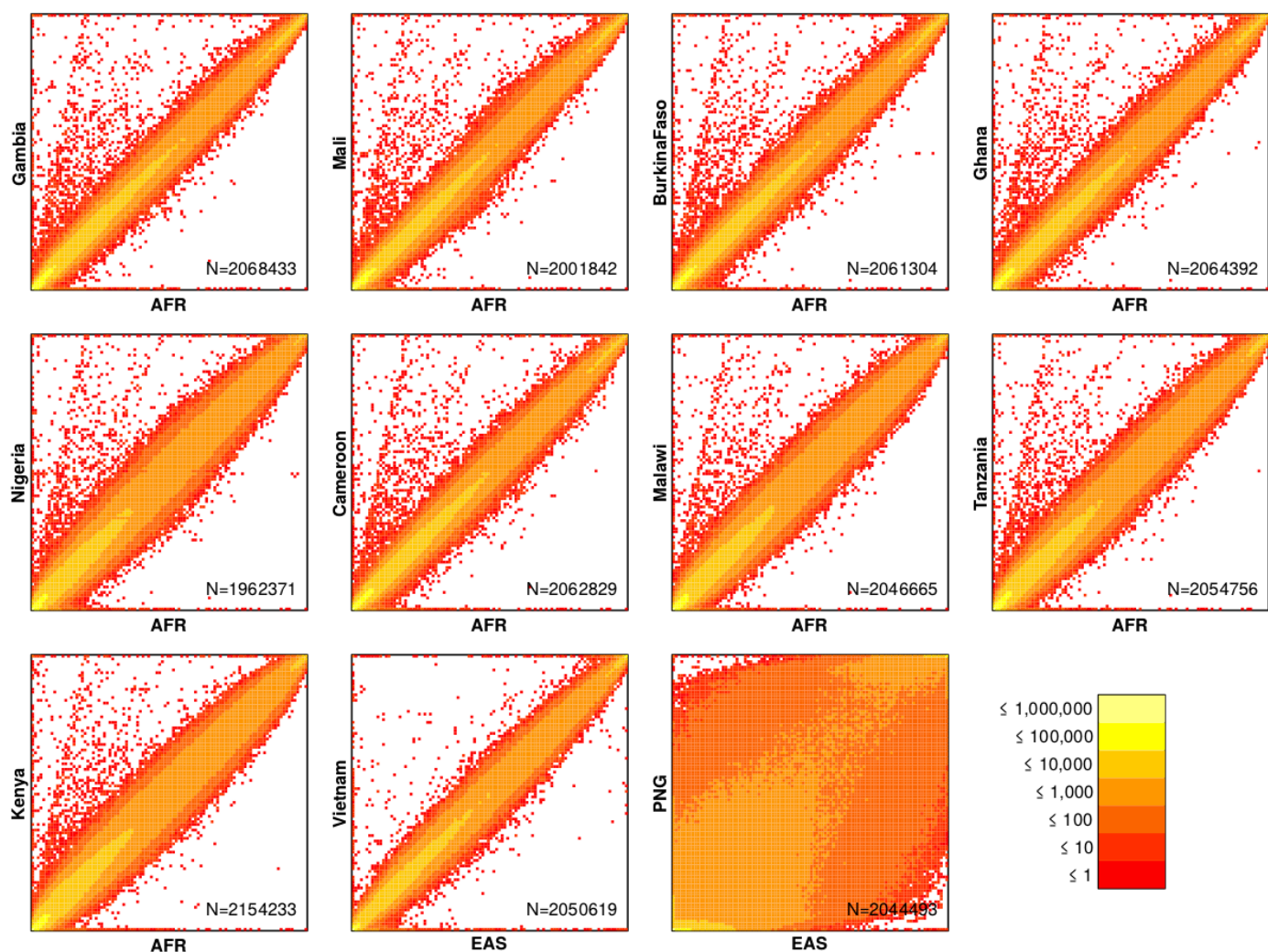
Supplementary Figure 11 - Evidence for within-Africa differentiation at variants across the genome

Plot shows the evidence for differentiation ($-\log_{10} P_{XtI}$, computed using controls from the 7 African study populations with at least 500 samples) at all variants with at least 2% mean allele frequency across the genome. Variants include genome-wide imputed SNPs, imputed HLA alleles, and glycoprotein CNVs. Table on right shows a set of variants selected to have $P_{XtI} < 1E-8$, and thinned such that no two variants lie within a distance of 0.5cM with a 25kb margin of each other (thinned separately for imputed HLA alleles and genome-wide variants). For each variant we show the ID, chromosome and position and the $-\log_{10} P_{XtI}$. Circles show the allele frequencies, with the area of each circle reflecting the minor allele frequency in proportion to the maximum minor allele frequency across African populations (shown as grey circle). Genes shown are the closest protein-coding genes that appear within the corresponding thinning region; asterisk denotes that the variant lies in the gene, and ellipsis indicates that further genes (not shown) lie within the region.



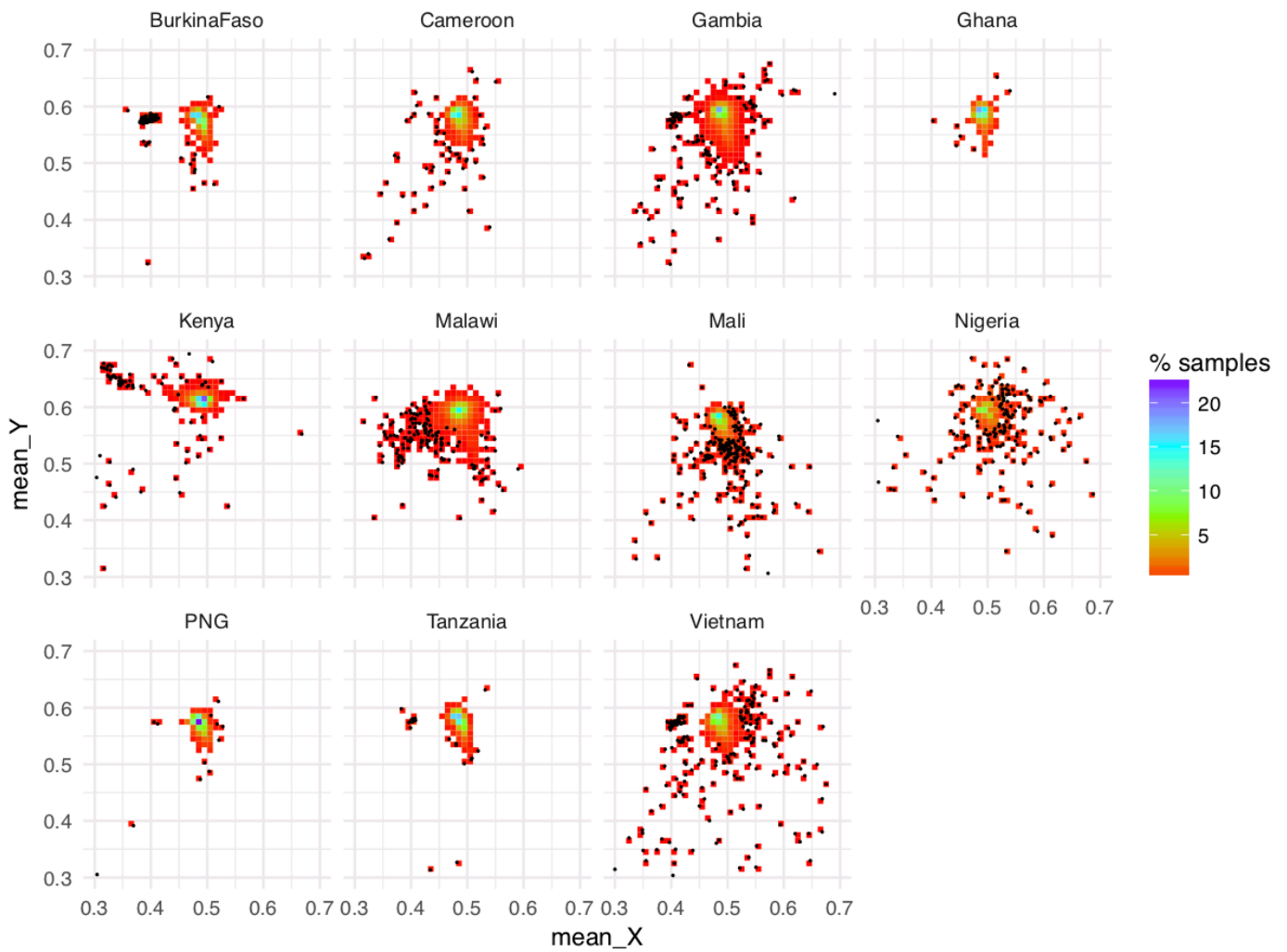
Supplementary Figure 12 - Mendelian randomization analysis with 36 haematopoietic traits

Results depict mendelian randomization analysis against each of 36 traits analysed in Astle et al, Cell (2017). Points show the Mendelian randomization analysis of SM and each trait, at 2130 'sentinel' SNPs from Astle et al and having association results in our study. The estimated correlation and P-value are shown in blue. Traits are ordered by p-value from lowest to highest. For further details see **Methods** and the legend for **Fig. 5h**.



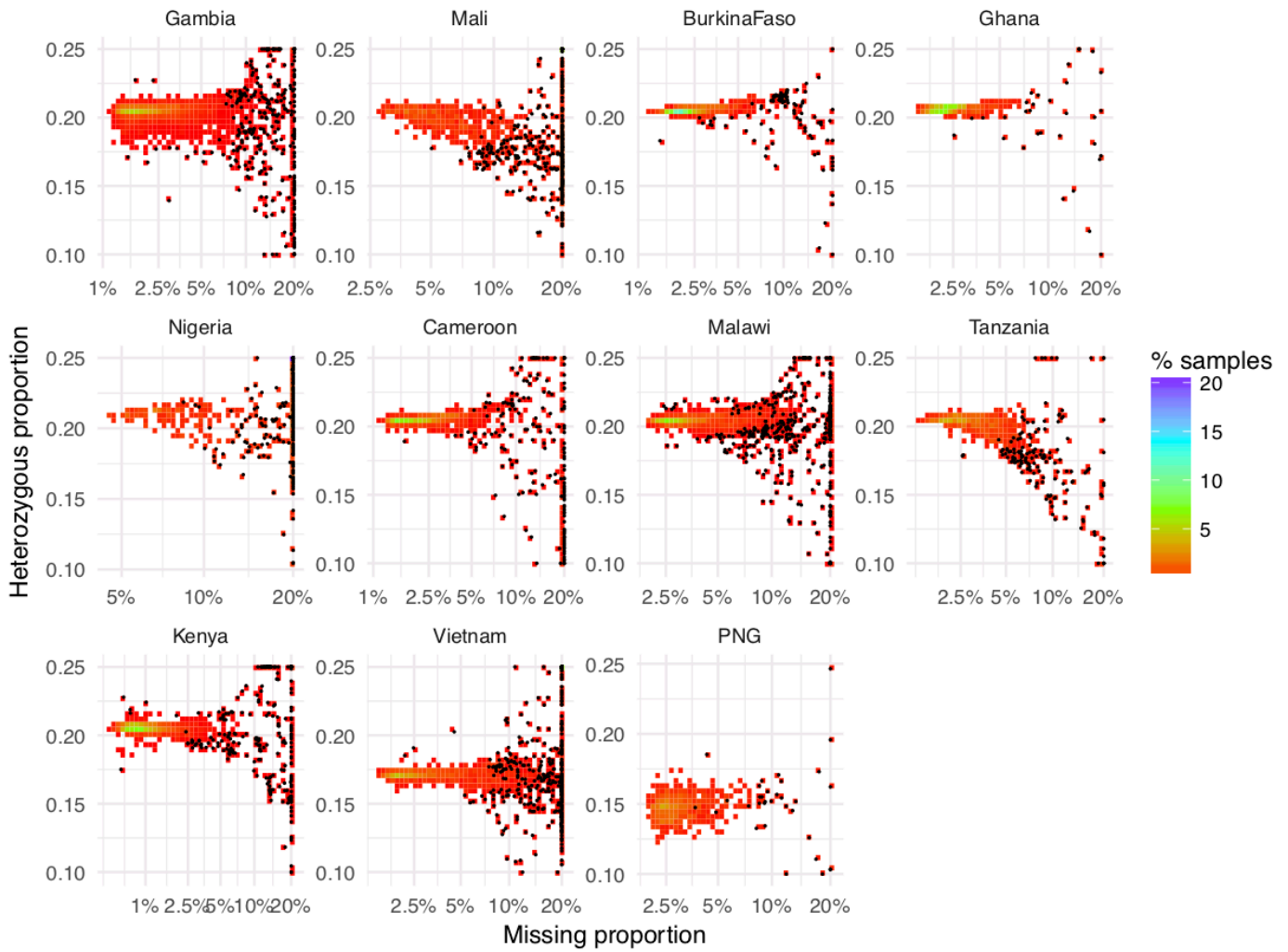
Supplementary Figure 13 - Comparison of reference panel and study frequencies at typed SNPs

Figure shows the distribution of non-reference allele frequencies for SNPs on the Omni 2.5M platform after data alignment. The X axis denotes the frequency in the closest reference panel group, which is AFR for African populations and EAS for non-African study populations. Only SNPs with missing proportion < 10% in each study population, and that are also present in the combined reference panel (as identified by genomic position and alleles) are shown. Numbers in text denote the total number of SNPs plotted, and colours denote the counts in each cell according to the legend at the bottom right.



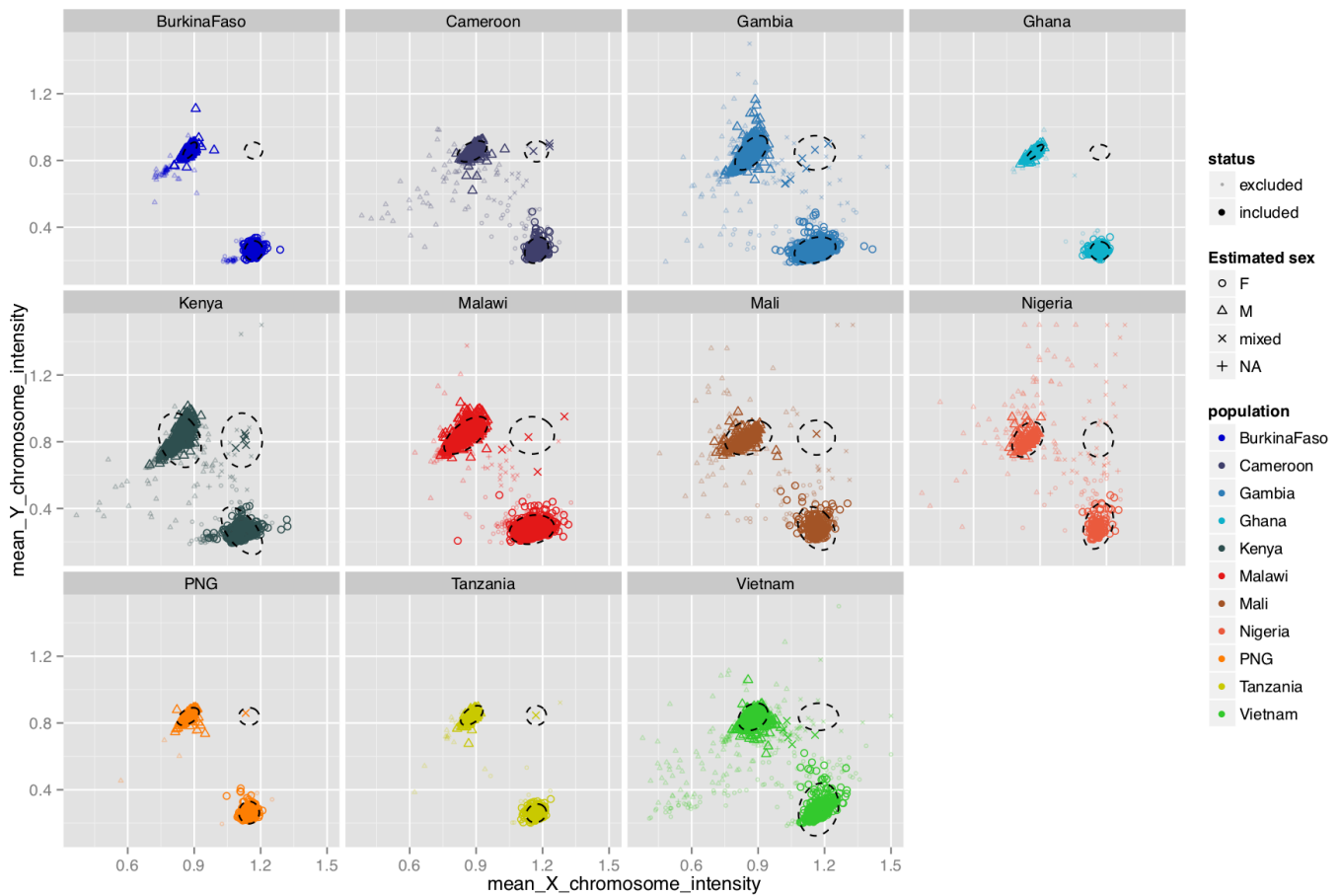
Supplementary Figure 14 - Average X and Y channel intensity values per sample in each population, and intensity exclusions.

Heatmaps show the proportion of samples in each site with the given average intensity values. Excluded samples were computed using ABERRANT and are shown as black dots.



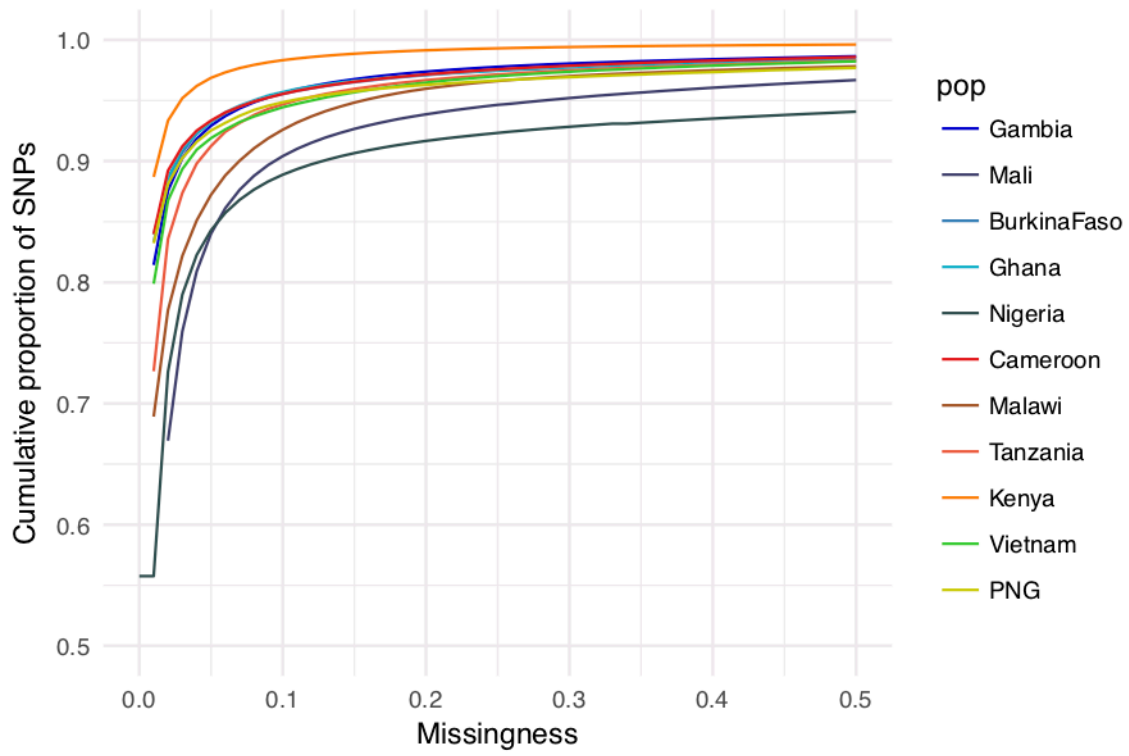
Supplementary Figure 15 - average missing call and heterozygosity rates per sample, and sample exclusions.

Heatmaps show the proportion of samples in each population with the given average missing call rate (on a logit scale, x axis) and average heterozygosity (y axis). Exclusions were computed using ABERRANT and are shown in black dots.



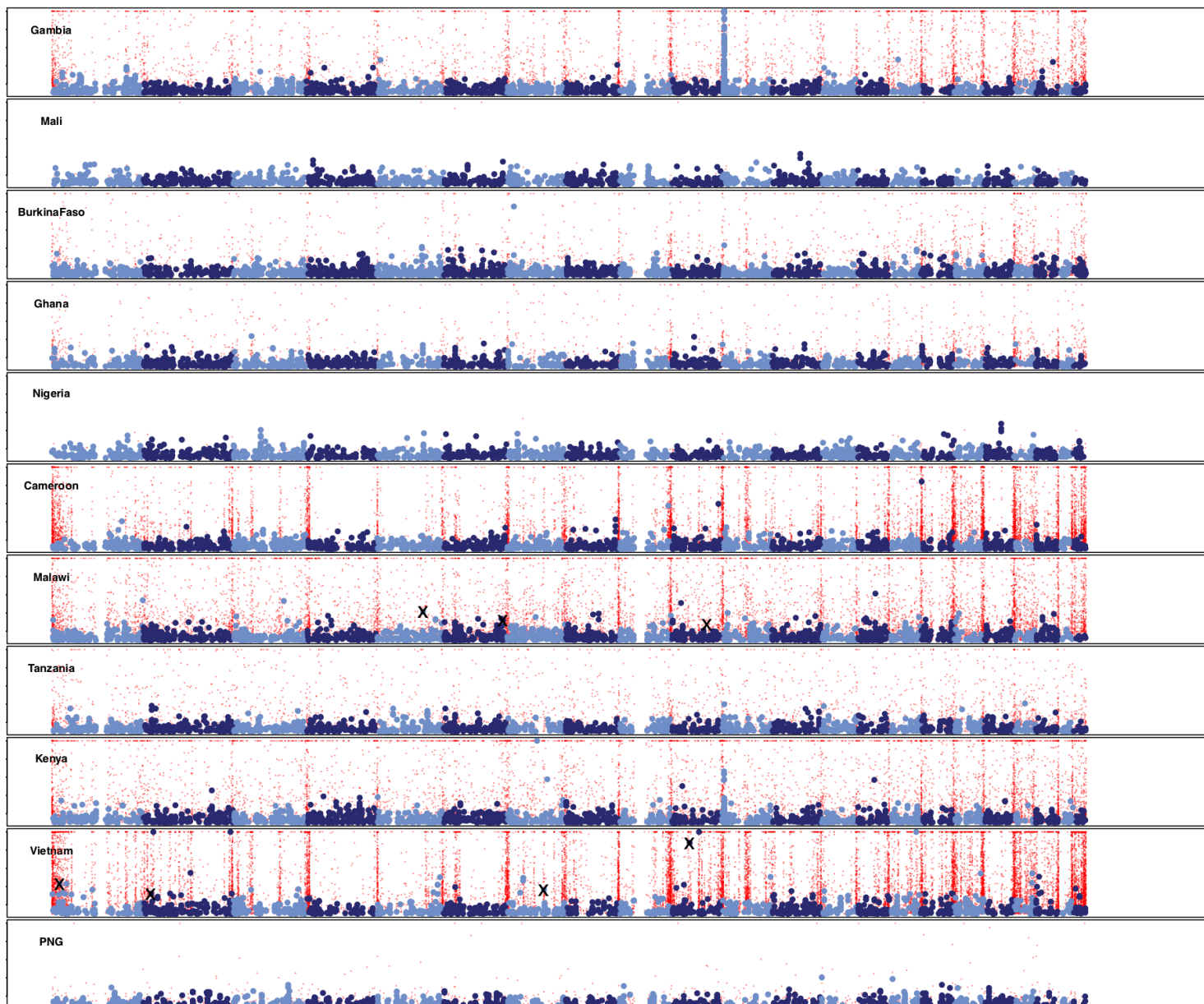
Supplementary Figure 16 - Average X+Y channel intensities across sex chromosomes, and gender assignment.

Plot shows total (X channel + Y channel) intensity averaged across X chromosome variants (x axis) and Y chromosome variants (y axis) for each sample, computed using normalized intensities from the Omni 2.5M platform. Shapes denote the gender assignment of each sample, and are estimated using the cluster positions denoted with dashed ellipses. Excluded samples are shown as smaller, transparent points.



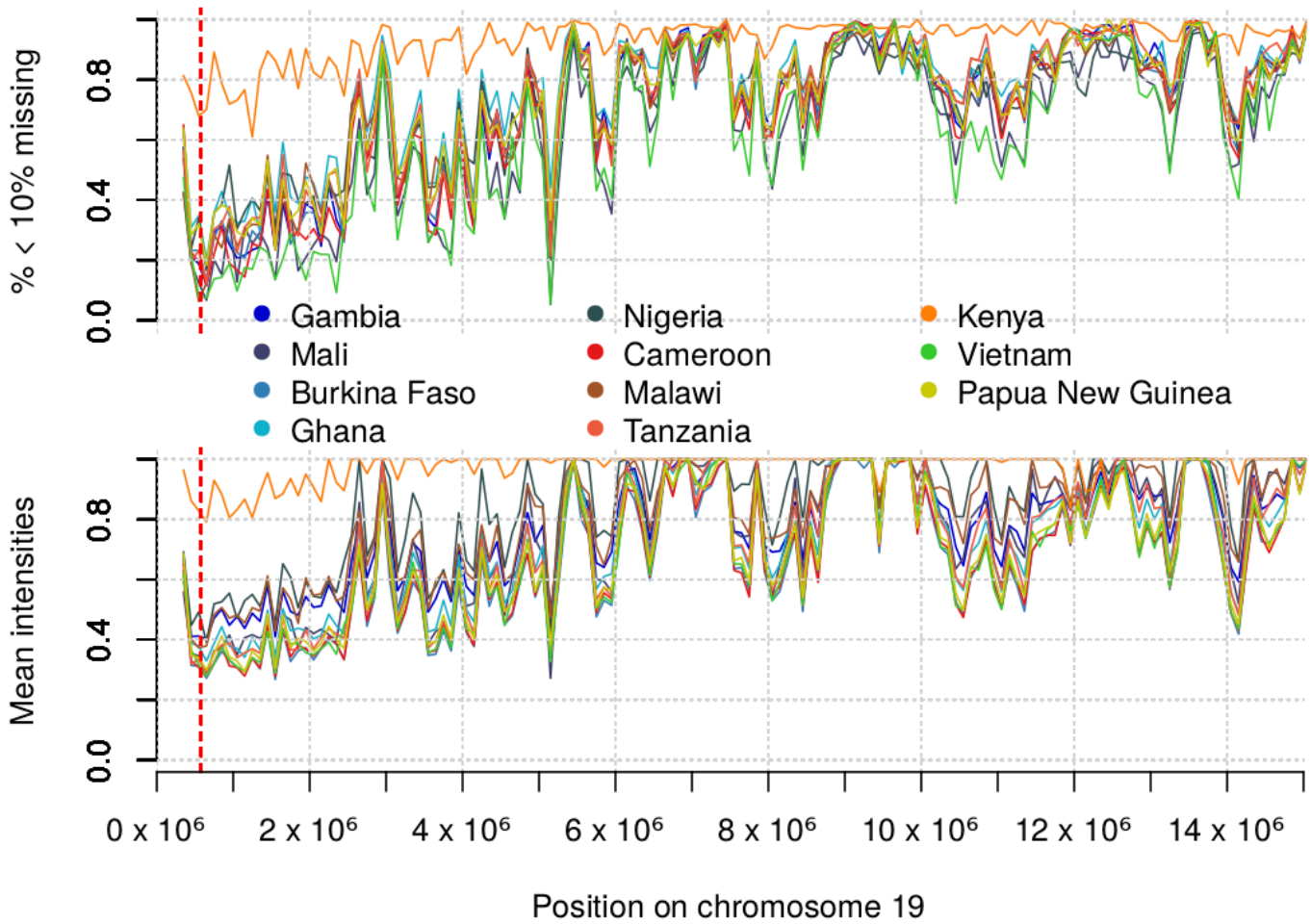
Supplementary Figure 17 - cumulative distribution of per-sample missingness.

Plot shows the proportion of samples in each study population (y axis) that has less than a given rate of missingness (indicated by the x axis), across all at SNPs on the Omni 2.5M platform after data alignment.



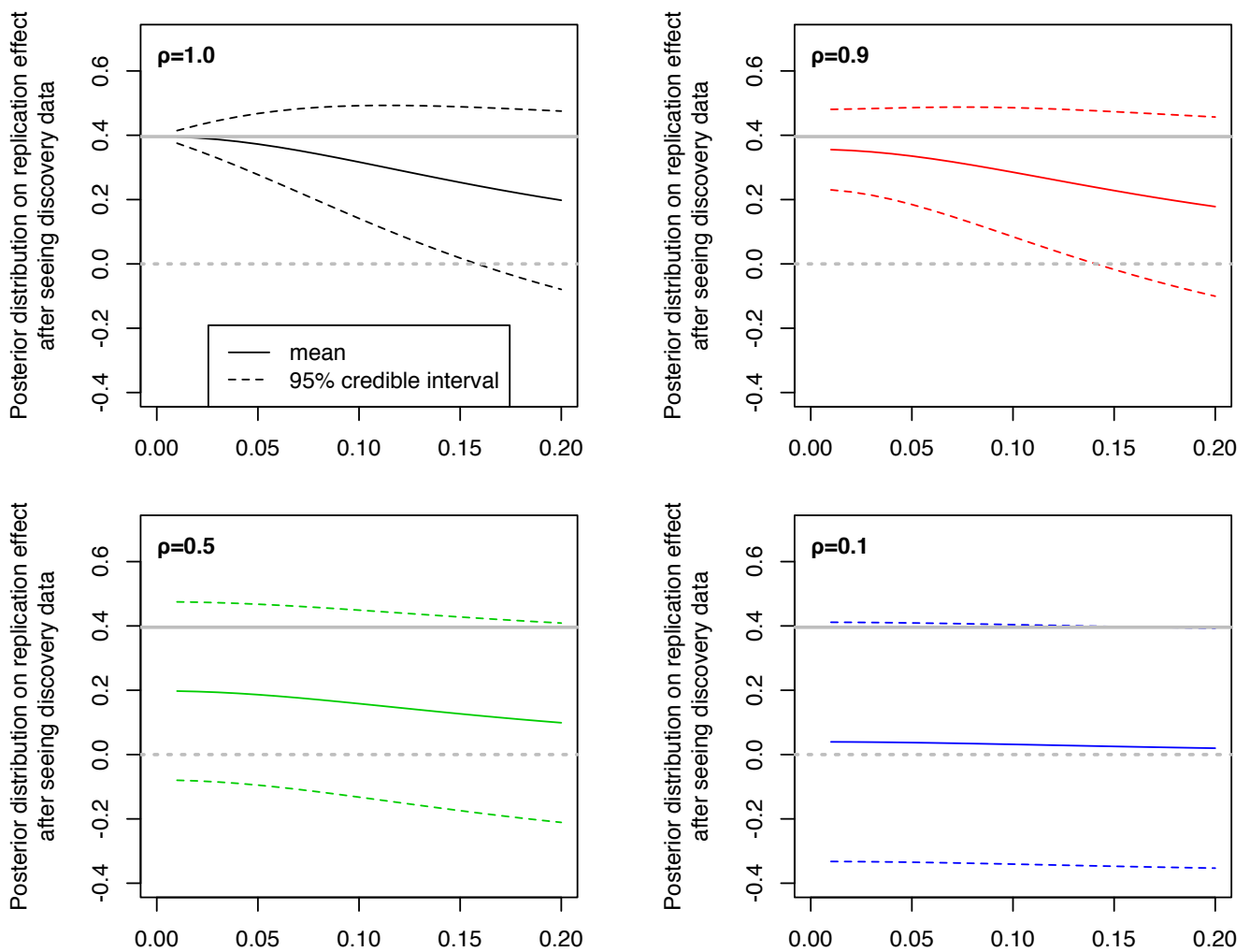
Supplementary Figure 18 - Detail of QC: manhattan plots.

Rows show manhattan plots for association of severe malaria with directly-typed SNPs, under a general model of association. Red points denote SNPs that were removed during our QC process. Black crosses denote SNPs that were manually removed after inspection of cluster plots.



Supplementary Figure 19 - Array intensities and genotyping near the end of chromosome 19

Top panel shows the percentage of variants on the Omni 2.5M microarray which had at least 10% missing calls in our data, for each study population (colours), computed in 100kb bins across the chromosome. Second panel shows the total (X channel+Y channel) intensity for the same SNPs, averaged over 100kb bins. The vertical dashed red line depicts the location of the *BSG* gene.



Supplementary Figure 20 - Illustration of replication effect size model.

Figure shows the modeled distribution of replication effect sizes, given a specific effect size observed in discovery as described in **Supplementary Note 5**. We assume a discovery log odds ratio of $0.396 = \log(1.49)$ (solid horizontal grey line) with standard error indicated by the x axis. Solid / dashed coloured lines indicate the mean and 95% credible interval of the true effect in replication. For this plot a marginal prior distribution with mean 0 and standard deviation 0.2 is assumed for discovery and replication effects, with correlation given by ρ (figure label).

Supplementary Tables

Country	Institute	Ethics approving institution	Ethics committee	local ID(s) Case-Control Study	localID(s) Whole-genome sequencing
Gambia	Medical Research Council Unit, The Gambia	MRC Gambia and Gambia Government	MRC/Gambia Government Ethics Committee	SCC 1029v2 SCC670/630	SCC1156v2
Mali	University of Bamako	University of Bamako, FMPOS, MRTC	FMPOS Research Ethics committee	No/18/FMPOS No/06-18bis/FMPOS	NA
Burkina Faso	Centre National de Recherche et de Formation sur le Paludisme	Ministry of Health & Ministry of Science and Education	Health Research Ethics Committee	No 2007-048	No 2007-048
Ghana (Navrongo)	Navrongo Memorial Institute for Medical Research with Navrongo Health Research Centre	Navrongo	Navrongo Institutional Research Committee	NMIMR-IRB CPN 016/01-02; NMIMR-IRB CPN 029/05-06	NA
		Ghana Health Service	Ghana Health Service Ethics Research Board	GHS-ERC-03/9/06	
Ghana (Kumasi)	Kwame Nkrumah University of Science and Technology	School Medical Sciences, KNUST	Committee on Human Research Publication and Ethics	CHRP/07/01/06 CHRPE SMS UST dated 24-05-2007	NA
Nigeria	University of Ibadan (UI)	Institute of Child Health, College of Medicine, University of Ibadan	UI/UCH Ethics committee	UI/IRC/06/0034	NA
Cameroon	University of Buea	University of Buea	Institutional Research Board	University of Buea ethical clearance 07-12-2005	University of Buea ethical clearance 10-12-2005
		Government of Cameroon	Provincial Delegate for Public Health	D7.1.A/MPH/SWP /PDPH/PS.CH/234 0/811	D7.1.A/MPH/SWP/P DPH/PS.CH/2340/811
Kenya	KEMRI-Wellcome Research Programme	KEMRI, Kilifi	KEMRI Research Ethics Committee	SCC1192	
Tanzania	Joint Malaria Programme, Kilimanjaro Christian Medical Centre	London School of Hygiene and Tropical Medicine	London School of Hygiene and Tropical Medicine Ethics Research Committee	4093	4093
		National Institute for Medical Research (NIMR), Tanzania	NIMR Research Coordinating Committee	NIMR/HQ/R.8a/Vol. IX/513	NIMR/HQ/R.8a/Vol. IX/611
Malawi	Blantyre Malaria Project with Malawi-Liverpool-Wellcome Programme	University of Malawi, College of Medicine	College of Medicine Research Ethics Committee	P.05/06/442	NA
Viet Nam	Oxford University Clinical Research Unit	Hospital Tropical Diseases	Research Ethics Committee	SECHTD dated 20/04/2006	NA
Papua New Guinea	Papua New Guinea Institute for Medical Research	Government of PNG	Papua New Guinea Medical Research Advisory Committee	MRAC No:06.21	NA
		Papua New Guinea Institutional Research Board	Papua New Guinea Institute of Medical Research Institutional Research Board	IMR IRB 0603	
United Kingdom	Oxford University	Oxford University	The Oxford Tropical Research Ethics Committee (OXTREC)	OXTREC 020-06	

Supplementary Table 1 - Detail of partner studies and ethics approval.

Partner sites for MalariaGEN Consortial Projects 1 and 3 and the Gambian Genome Variation Project with details of the partner institution and local approving bodies.

Country	Previous publications (candidate variant typing)	Previous publications (microarray data)	Previous publications (sequencing data)
Gambia	MalariaGEN ^{1,2} , Shah et al ³ , Clarke et al ⁴	Jallow et al ⁵ ; Band et al ⁶ ; MalariaGEN ¹ ; Leffler et al ⁷ ; Busby et al ⁸	Leffler et al ⁷
Mali	MalariaGEN ^{1,2} , Toure et al ⁹ , Clarke et al ⁴	Busby et al ⁸	
Burkina Faso	MalariaGEN ^{1,2} , Clarke et al ⁴	Busby et al ⁸	Leffler et al ⁷
Ghana	MalariaGEN ^{1,2} , Clarke et al ⁴	Busby et al ⁸	-
Nigeria	MalariaGEN ^{1,2} , Olaniyan et al ¹⁰ , Clarke et al ⁴	Busby et al ⁸	-
Cameroon	MalariaGEN ^{1,2} Apinjoh et al ^{11,12} , Clarke et al ⁴	Busby et al ⁸	Leffler et al ⁷
Malawi	MalariaGEN ^{1,2} , Clarke et al ⁴	Band et al ⁶ ; MalariaGEN ¹ ; Busby et al ⁸ ; Leffler et al ⁷ ;	-
Tanzania	MalariaGEN ^{1,2} ; Manjurano et al ¹³⁻¹⁵ , Clarke et al ⁴ ; Supulveda et al ¹⁶	Busby et al ⁸ ; Ravenhall et al ¹⁷	Leffler et al ⁷ ; Ravenhall et al ¹⁷
Kenya	MalariaGEN ^{1,2} ; Opi et al ¹⁸ ; Ndila et al ¹⁹ ; Shah et al ²⁰ ; Ugoya et al ²¹ ; Clarke et al ⁴ ; Mackinnon et al ²² ; Kariuki et al ²³ ; Muriuki et al ²⁴	Band et al ⁶ ; MalariaGEN ¹ ; Busby et al ⁸ ; Leffler et al ⁷	Leffler et al ⁷
Vietnam	MalariaGEN ^{1,2} , Dunstan et al ²⁵ , Clarke et al ⁴	-	-
Papua New Guinea	MalariaGEN ^{1,2} , Manning et al ²⁶ , Clarke et al ⁴	-	-

Supplementary Table 2 - Previous publications

The first column lists study countries. The last three columns refer to papers published by consortium members using data generated by this project. This includes publications using direct typing of candidate variants, publications on genome-wide microarray data, and publications using short-read sequencing data.

Collection		Pre-phasing					Post-phasing	
Population	Total samples analysed (repeats)	Intensities	Miss / het	Gender	Duplicates / repeats	TOTAL	Relatedness (PCs, non-cases-control sample)	TOTAL
Gambia	5594	137	182	4	99	5171	192 (1)	4979
Mali	900	220	191		2	484	52 (3, 10)	422
Burkina Faso	1446	69	28		20	1325	31 (4)	1294
Ghana	782	7	25		14	732	11 (3, 15)	706
Nigeria	419	192	84		8	133	0 (2)	133
Cameroon	1471	64	118	3	9	1272	55 (5)	1217
Malawi	2791 (297)	150	250	3	186	2495	24 (4)	2471
Tanzania	979	22	126	1	11	814	16 (5)	798
Kenya	3769 (96)	120	116	6	156	3462	355 (5, 39)	3068
Vietnam	1690 (38)	263	174	1	26	1260	13 (4)	1247
PNG	815	12	21	1	5	772	51 (4)	721
TOTAL	20,656 (431)	1,257	1,315	19	536	17,960	800 (40, 64)	17,056

Supplementary Table 3 - Detail of Sample QC

'Collection' columns show: the population label (PNG denotes Papua New Guinea); total samples analysed per study population (all samples, including repeat samples that were included in the QC process). 'Pre-phasing' columns show: samples removed due to outlying intensities, outlying missingness/heterozygosity, unassigned gender, or due to being identified as a duplicate/repeat of another sample, and the total number of samples included in phasing. 'Post-phasing' columns show: the number of samples excluded from association testing due to being closely related to other samples (estimated relatedness > 0.2), identified as outlying on principal components, or lacking case/control status (e.g. for parent samples) where applicable; and the total included in association testing.

Popula- tion	Total SNPs	Missing- ness	frequency	HWE / MF	plate	Recall	Cluster / platform	TOTAL
<i>Autosomes</i>								
Gambia	2,312,228	163,463	457,765	2,129	5,082	646		
Burkina Faso	2,312,228	156,296	464,801	75	3,242	34		
Ghana	2,312,228	156,576	446,825	14	2,720			
Came- roon	2,312,228	153,740	451,465	69	2,824	22		
Malawi	2,312,228	171,305	461,725	1,022	12,771	2361		
Tanzania	2,312,228	123,024	458,999	45	4,003	155		
Kenya	2,374,031	132,070	480,658	382	3,296	20		
Vietnam	2,312,228	187,266	927,210	30	1,953	17,126		
PNG	2,312,228	246,303	1,017,977	19	1,929			
Combined	2,383,648	426,545	289,371	1,315	28,026	36,823	6/51,048	1,550,514
<i>X chromosome</i>								
Gambia	55,510	5,138	8093	753	249			
Burkina Faso	55,510	4,154	8,313	441	234			
Ghana	55,510	4,301	8,120	221	439			
Came- roon	55,510	4,191	8,547	587	135			
Malawi	55,510	6,174	8,419	830	216			
Tanzania	55,510	3,746	8,186	185	354			
Kenya	57,044	6,351	8,563	569	179			
Vietnam	55,510	6,185	19,489	278	247			
PNG	55,510	6,851	21,632	251	219			
Combined	57,104	13,740	4,719	224	2,331	-	2,695	33,395

Supplementary Table 4 - Detail of SNP QC

Columns show: the population label, total number of SNPs genotyped, SNPs removed due to missingness in each population, SNPs additionally identified as low frequency, out of Hardy-Weinberg equilibrium, or failing the plate or recall test in each population. PNG denotes Papua New Guinea. The 'Combined' rows show the total number of SNPs and the number failing each combined filter, including the criteria of at least two populations with frequency > 1%. For the X chromosome, missingness and plate test were computed separately in males and females, and a test of difference in frequency between males and females was used in place of HWE.

Category	Short name	Detail	Prior weight
<i>Mode of inheritance</i>			
Additive	add	Encoded as AB+2*BB	0.4
Dominant	dom	Encoded as AB+BB	0.2
Recessive	rec	Encoded as BB	0.2
Heterozygote	het	Encoded as AB	0.2
TOTAL			1
<i>Population</i>			
Fixed effects	fix	All off-diagonal entries of P are set to 0.99	0.4
Correlated effects	cor	All off-diagonal entries of P are set to 0.9	0.2
Independent effects	ind	All off-diagonal entries of P are set to 0	0.04
Structured effects	str	Uses P estimated from the correlation in allele frequencies genome-wide	0.04
Population group-specific effects		Effects assumed to be restricted to a subset of populations.	0.04 per subset. 8 subsets in total as detailed in Methods .
TOTAL			1
<i>Subphenotype effects</i>			
Case/control effects		(models as described above)	0.8
Correlated between subphenotypes	cm-sma-other-cor	Between-phenotype entries of P set to 0.9	0.04
Independent across subphenotypes	cm-sma-other-ind	Between-phenotype entries of P set to 0	0.04
Effects restricted to two subphenotypes		σ nonzero for two phenotypes	0.02 per pair of subphenotypes
Effects restricted to one phenotype		σ nonzero for one phenotype	0.02 per subtype
TOTAL			1

Supplementary Table 5 - Detail of models included in BF_{avg}

The table shows the component models included in the model-averaged Bayes factor. Columns specify the model name and shortened mnemonic name, detail of the implementation, and the prior weight in the BF_{avg} . Prior weights are given per category; to compute the full prior weight for a model, weights should be multiplied across categories. For example, the model of dominant effects on cm and sma is weighted as $0.2 \times 0.02 = 0.004$. For subphenotype analysis, between-population correlation for each phenotype was set to 0.99, and between-population between-phenotype correlation was set to 0.99 times the assumed between-phenotype correlation.

Supplementary Notes

Supplementary Note 1 - Investigation of the HBA1-HBA2 region

Variation in the genes encoding alpha globin (*HBA1*, chr16:226679-227520; and *HBA2*, chr16:222846-223709) have been linked to malaria susceptibility as reviewed previously^{27,28}. In particular, the $-\alpha^{3-7}$ deletion, which deletes a 3.7kb sequence forming a hybrid *HBA2-HBA1* gene, is a cause of alpha thalassaemia and is found at nontrivial frequency in African populations. Alpha thalassaemia is thought to be protective against malaria, but direct evidence for this hypothesis is currently somewhat limited. Available evidence comes both from observation of the distribution across populations (reviewed in²⁹) and from direct testing of this variant in case/control samples (e.g. OR=0.83 (0.76–0.90); $P=2\times 10^{-6}$; observed using direct typing of N=6193 children in Kilifi, Kenya¹⁹; these samples are also included in our study).

We did not observe strong signal of association across the *HBA1-HBA2* region in our GWAS study (e.g. maximum $BF_{avg} = 31$ within the first megabase of chromosome 16, obtained at rs150383783 chr16:580412; maximum $BF_{avg} = 11$ within 100kb of *HBA1-HBA2*). The 1000 Genomes reference panel contains a variant identified from sequence reads that corresponds to the $-\alpha^{3-7}$ deletion (appearing in the panel as EM_DL_DEL34404, chr16:223678±150-227490±150, length = 3812; combined frequency = 5.5% across African ancestry samples in the 1000 Genomes project). In our data, EM_DL_DEL34404 was imputed at high frequency in all African populations (allele frequency = 8.5%, 10.0%, 15.0%, 16.7%, 17.1%, 19.1%, 30.7%, 27.4%, 31.5% in Gambia, Mali, Burkina Faso, Ghana, Nigeria, Cameroon, Malawi, Tanzania and Kenya respectively; frequency = 1.5% in Vietnam and <1% Papua New Guinea). Imputation confidence was also nontrivial (IMPUTE info = 0.73-0.86 in African study populations). However, we observed only modest evidence for association with EM_DL_DEL34404 ($BF_{avg} = 4.3$; fixed-effect additive $P_{add} = 0.002$; OR = 0.90; 95%CI = 0.84-0.96). The strongest evidence for association in individual populations was observed in Malawi (OR=0.83; 95%CI = 0.72-0.95; $P_{add}=0.007$).

These findings may be taken to confirm that $-\alpha^{3-7}$ confers a modest protective effect. However, we also noted reasons that suggest these results, based on imputation, should be treated with caution. First, the *HBA1-HBA2* region lies near the start of chromosome 16, and is susceptible to an observed end-of-chromosome effect on study genotype quality (described further in **Supplementary Note 2** below). This limits the amount of data informing on imputation, such that only 115 SNPs in our post-QC set lie in the region chr16:0-1,000,000.

Second, LD between EM_DL_DEL34404 and regional SNPs appears relatively weak and differs substantially between populations (max $r^2 = 0.53$ between EM_DL_DEL34404 and all other reference panel variants in the first megabase of chromosome 16; this maximum is attained at rs76462751 in the ESN and YRI populations; $r^2 = 0.001$ at the same SNP in GWD and < 0.25 in MSL and LWK; $r^2 < 0.4$ for all other SNPs except in ESN; no SNPs with $r^2 > 0.1$ in all African populations). This pattern of LD suggests that the $-\alpha^{3-7}$ deletion may be carried on several distinct haplotypes across populations, a situation which is naturally challenging for imputation-based approaches. (In particular, this appears incompatible with a hypothesis of a single recent origin and subsequent positive selection of $-\alpha^{3-7}$, but does appear consistent with the high observed de novo mutation rate of this deletion³⁰).

Finally, comparison of imputed $-\alpha^{3-7}$ genotypes to previously reported direct-typing in Kenya¹⁹ reveals a relatively low accuracy that is overestimated by the IMPUTE info score ($r^2=0.42$ between expected number of copies of $-\alpha^{3-7}$ inferred from imputation and copies inferred from direct typing, in N=2913 Kenyans; IMPUTE info = 0.86). These results do not take account of other, globally rarer thalassaemia-causing alleles. Greater accuracy of inference in this region will be of interest.

Supplementary Note 2 - Investigation of the basigin region

Basigin has been identified as a receptor for *P.falciparum* malaria during invasion of red blood cells, and the interaction between basigin and the Pf ligand PfRh5 is thought to be essential to the invasion process³¹. It is therefore plausible that the gene encoding basigin (*BSG*, chr19:572454-583493) might harbour genetic mutations that affect invasion and hence malaria infection outcomes. However, we found little signal of association across the region containing *BSG* (e.g. maximum $BF_{avg} = 48$ within 100kb of *BSG*, occurring at rs141173385 which is approximately 88kb upstream of *BSG*; maximum $BF_{avg}=3.8$ within 1kb of *BSG*). On closer inspection we noted that few typed SNPs in the region are contained in our set of QCd haplotypes (e.g. 67 typed SNPs after QC in the first megabase of chromosome 19, compared to approximately 420 per Mb across the whole of chromosome 19). We plotted SNP QC metrics in the first 15Mb of chromosome 19 (**Supplementary Figure 19**) and noted generally poor genotyping across the region. Specifically, we noticed lower-than average normalised array intensities and low rates of genotype calling across the first ~5Mb of chromosome 19. Similar, but less extreme issues were seen on other chromosomes and we suggest that this likely reflects issues with preparation of samples via whole genome amplification. The Kenyan study population, which was typed on the Omni 2.5M 'quad' platform, was affected by this issue but in a less extreme way than other populations.

Supplementary Note 3 - Investigation of association in *G6PD* and *CD40LG*

We have previously reported evidence of association within *G6PD*^{2,4} and upstream of *CD40LG*², both of which lie on the X chromosome, using direct typing of variants which are common in African populations. Here we compare these results to those based on our imputed data. Both rs1050828 (*G6PD* c.202C>T, chrX:153,764,217) and rs3092945 (chrX:135,729,609, upstream of *CD40LG*) were imputed with high confidence (info > 0.9) in all African populations. However, under our bayesian model average, evidence for association at both variants was weak ($BF_{avg} < 1$) and there was little evidence for association at variants across these regions ($BF_{avg} < 10$ within 100kb of rs1050828 or rs3092945), except for $BF_{avg} = 40$ at rs369388464, which lies in an intron of *ARHGEF6*).

We note two explanations for these results. First, the observed effects at rs1050828 in *G6PD* have been noted to be complex, with putative opposing effects in males and females (which would not be picked up by our analysis, which treats males like homozygous females for the purpose of association testing) and in severe malaria subtypes. We did note weak evidence for an SMA-only effect of rs1050828 ($BF = 6$ for SMA-only model; $OR_{SMA} = 1.3$, 95% CI 1.07-1.71, $P = 0.01$; $OR_{CM} = 0.96$). These results are thus consistent with previous estimates based on direct typing in these samples^{2,4}, though we did not observe evidence for a protective effect on CM in this analysis.

Second, we noted some evidence at both SNPs of discrepancies between direct typing and imputation in specific populations. Specifically, at rs1050828, correlation between imputed and directly-typed genotypes was > 0.9 in all African study populations except The Gambia ($r^2 = 0.73$). At rs3092945 we also found discrepancies in The Gambia ($r^2 = 0.73$) and Kenya ($r^2 = 0.8$). This is particularly notable because the reported signal of association is driven by strong and opposing observed effects in The Gambia and in Kenya, with little evidence in other populations. Inspection of directly-typed data suggests that the directly-typed rs3092945 is out of Hardy-Weinberg equilibrium in the Gambia and other populations. Our tentative interpretation is that the imputation is likely accurate, and the observed association may be at least in part driven by typing artifacts.

Supplementary Note 4 - Analysis of functional annotations

We reasoned that functional annotations might provide clues to further true associations among our list of most associated regions, as well as to the likely causal variants within these regions. To assess this, we examined functional annotations of all variants (described in Methods) with modest or strong evidence of association (defined as having $BF_{avg} \geq 100$ and lying in the 95% credible set of a lead variant with $BF_{avg} \geq 1000$, under the assumption of a single variant within the association region³²). These results are listed in **Supplementary Data 3**.

Outside the human leukocyte antigen region (HLA), six protein-altering mutations lie in this list: the HbS and O blood group mutations (**Figure 2c**), which are the sole members of their 95% credible sets, and SNPs in the aminoacyl-tRNA synthetase *IARS* (rs2070053, $BF_{avg}=1.1 \times 10^3$), the olfactory receptor OR4N5 (rs149008519, $BF_{avg} = 623$), the ankyrin repeat-containing *ANKRD30B* (rs9748611, $BF_{avg}=394$), and in *ECM2* (rs41278707, $BF_{avg} = 175$). The derived ('A') allele at rs2070053 is at only 1-2% frequency and is predicted to have a strong risk effect in our data ($OR_{add}=1.64$, 95% CI=1.32-2.04), but its effect on the protein is reported to be benign³³. rs149008519 and rs41278707 are also relatively rare (1-2% in African, and < 0.2% in non-African populations in our data). The derived 'A' allele at rs9748611 is more common, but has a complex observed pattern of effects across populations, such that it appears protective in Kenya and Gambia ($OR_{het} = 0.79$, 95% CI = 0.66-0.95 in the Gambia; $OR_{het} = 0.6$, 95% CI = 0.49-0.74 in Kenya) but with opposing effects observed in other populations including Malawi ($OR_{het} = 1.2$, 95% CI = 0.96-1.50). None of these SNPs appear to have other trait associations at present. (We note also that the copy number variant DUP4, which we have found to underlie the association in the glycoporphin region, affects protein coding sequence through structural rearrangement of the underlying region.)

A number of regions also contain SNPs with evidence of potentially regulatory effects. We note here variants with multiple lines of evidence - namely those with evidence of eQTL effects, which also lie in an annotated transcription factor binding site, and which have previously been associated to other traits. This list includes the associations in *ATP2B4*, and at rs2523650 in the HLA, which are described in main text. Also, an associated eQTL for *VAC14* (rs8060947, $BF_{avg}= 550$), which encodes a component of the PIKFYVE complex, has recently been associated with *S.Typhi* invasion in vitro³⁴, with susceptibility to typhoid³⁵ and with some forms of bacteraemia³⁶, putatively through altering expression of *VAC14* with downstream effects on cholesterol.

Within the HLA we also noted a number of further potentially functional mutations with some evidence of association - including missense mutations in *HLA-C* (e.g. the missense mutations rs41549413 and rs41548123, $BF_{avg} = 144$) and reported eQTLs (rs9264638, $BF_{avg} = 636$).

The combined evidence of function and association with susceptibility to malaria at some of these loci may be considered of interest. However, complicating the results above is that neither the main signal in the HLA region nor that at *VAC14* appear to replicate in our additional replication samples (**Supplementary Data 1**).

Supplementary Note 5 - Bayesian analysis of replication

Replication analysis for a single association model

Consider assessing the evidence for association under a single model of association (denoted M_1 , parameterised by a vector of parameters θ) versus the model of no association (denoted M_0 , corresponding to $\theta \equiv \theta_0$), and suppose we have two tranches of data - a discovery set D_1 and a replication set D_2 . We assume these are sampled independently i.e. are conditionally independent given the true parameter value. The overall evidence in the data for M_1 , relative to M_0 , is expressed in the Bayes factor

$$BF^{\text{overall}} = \frac{P(D_1, D_2 | M_1)}{P(D_1, D_2 | M_0)} = \frac{\int_{\theta} P(D_1 | \theta) P(D_2 | \theta) P(\theta | M_1)}{P(D_1 | M_0) \cdot P(D_2 | M_0)} \quad (1)$$

where θ represents the parameters of M_1 (i.e. the genetic effect sizes). Since the Bayes factor based only on discovery data is

$$BF^{\text{discovery}} = \frac{\int_{\theta} P(D_1 | \theta) P(\theta | M_1)}{P(D_1 | M_0)}$$

multiplying and dividing by $BF^{\text{discovery}}$ gives

$$BF^{\text{overall}} = BF^{\text{discovery}} \cdot \int_{\theta} \left(\frac{P(D_2 | \theta)}{P(D_2 | M_0)} \cdot d_1(\theta) \right) \quad (2)$$

where $d_1(\theta)$ is the posterior mass on parameter value θ given the discovery data,

$$d_1(\theta) = P(\theta | D_1, M_1) = \frac{P(D_1 | \theta) P(\theta | M_1)}{\int_{\theta'} P(D_1 | \theta') P(\theta' | M_1)}$$

The second term in Supplementary Equation (2) can be interpreted as the evidence for M_1 versus M_0 in the replication data, given the effect size distribution learnt from the discovery data. We denote this quantity by $BF^{\text{replication}}$ so that

$$BF^{\text{overall}} = BF^{\text{discovery}} \cdot BF^{\text{replication}} \quad (3)$$

Supplementary Equation (3) is a basic reflection of the consistency of bayesian reasoning, in the sense that inference is unaffected by whether all data is treated together (as in the left hand side), or in tranches (as in the right hand side). This is an intuitively obvious property but we note that no similar property holds for commonly-used frequentist assessments of replication, since there is no simple relationship between the P-value computed across all data and those computed in discovery and replication samples separately. (We note that $BF^{\text{replication}}$ is not the same as the Bayes factor that would be computed in replication data using the original prior effect size distribution, i.e. ignoring the discovery data.)

Replication analysis using model averaging

Now suppose M_1, \dots, M_K are K models of association with prior weights

$$w_i = P(M_i | \text{variant is associated}) \quad \sum_i w_i = 1$$

Then the overall evidence for association can be assessed by summing over models,

$$BF_{\text{avg}}^{\text{overall}} = \sum_i w_i \cdot BF_i^{\text{discovery}} \cdot BF_i^{\text{replication}}$$

Again, multiplying and dividing by the discovery model-averaged Bayes factor $BF_{\text{avg}}^{\text{discovery}}$ gives

$$BF_{\text{avg}}^{\text{overall}} = BF_{\text{avg}}^{\text{discovery}} \cdot \sum_i \left(\frac{w_i \cdot BF_i^{\text{discovery}}}{\sum_j w_j BF_j^{\text{discovery}}} \right) \cdot BF_i^{\text{replication}}$$

The term in the bracket is the posterior weight on model M_i given the discovery data, conditional on one of the models of association being true. We write w'_i for this posterior weight and note it is simply computed by renormalising discovery data Bayes factors. With this convention, the discovery and replication evidence can be summarised in three quantities:

1. A model-averaged discovery Bayes factor based on a chosen set of prior weights,

$$BF_{\text{avg}}^{\text{discovery}} = \sum_i w_i BF_i^{\text{discovery}}$$

2. A model-averaged replication Bayes factor based on posterior weights and effect size distributions learnt from discovery data,

$$BF_{\text{avg}}^{\text{replication}} = \sum_i w_i' BF_i^{\text{replication}}$$

3. An overall model-averaged Bayes factor, which decomposes as a product of the two terms above

$$BF_{\text{avg}}^{\text{overall}} = BF_{\text{avg}}^{\text{discovery}} \cdot BF_{\text{avg}}^{\text{replication}} \quad (4)$$

Specifically, $BF_{\text{avg}}^{\text{overall}}$ may be interpreted as the overall evidence for association (conditional on the prior assumptions), while $BF_{\text{avg}}^{\text{replication}}$ may be interpreted as the evidence that the effect, as learnt in the discovery data, replicates in the independent replication samples.

In our implementation we use the approximate Bayes factor formulation to compute $BF_{\text{avg}}^{\text{discovery}}$ and $BF_{\text{avg}}^{\text{overall}}$, given the maximum likelihood estimate and standard error computed separately in discovery and replication samples in each population, as described in Methods. We then use Supplementary Equation (4) to compute $BF_{\text{avg}}^{\text{replication}}$ as the ratio of the two. However, as described below, we additionally modify this computation to be more lenient about observed differences in effect size between discovery and replication data.

Allowing for deviation in effect size between discovery and replication

The method outlined above assumes that true replication effect sizes are identical to those learnt in discovery, and may be too restrictive in practice for several reasons. Firstly, phenotyping may differ between discovery and replication samples. This is the case in our data, where samples with strict phenotype definitions (CM and SMA) were preferentially picked for discovery typing, subject to sufficient DNA quantities. Second, in the context of GWAS, Winner's curse will lead to preferential choice of variants with large observed effect sizes, leading to over-estimation of effect sizes in discovery. Third, the potential for differences in genotyping behaviour between discovery and replication cohorts, e.g. due to technology differences or imputation, may also lead to discrepancies.

To allow for this, we modify formula Supplementary Equation (2) by additionally allowing the true replication effects to differ from those in discovery. Formally, we split the parameter θ into a parameter θ_1 (the true effects in discovery) and θ_2 (the true effects in replication), and write

$$\begin{aligned} BF^{\text{overall}} &= \frac{P(D_1|M_1)P(D_2|D_1,M_1)}{P(D_1|M_0)P(D_2|M_0)} \\ &= BF^{\text{discovery}} \cdot \frac{\int_{\theta_2} P(D_2|\theta_2)P(\theta_2|D_1)}{P(D_2|M_0)} \\ &= BF^{\text{discovery}} \cdot \int_{\theta_2} \left(\frac{P(D_2|\theta_2)}{P(D_2|M_0)} \cdot \int_{\theta_1} P(\theta_2|\theta_1)d_1(\theta_1) \right) \end{aligned} \quad (5)$$

For replication analysis, we further assume that θ_1 and θ_2 have a prior joint multivariate normal distribution with zero mean and variance of the form

$$\begin{pmatrix} \Sigma & \rho\Sigma \\ \rho\Sigma & \Sigma \end{pmatrix}$$

where Σ reflects the association model for discovery phase, as described in Methods, and ρ is a correlation coefficient. This implies that

$$P(\theta_2|\theta_1) = \mathcal{M}\mathcal{V}\mathcal{N}(\rho\theta_1; (1-\rho^2)\Sigma)$$

In our approximate framework the posterior distribution of effect sizes given discovery data, $d_1(\theta_1)$, is also multivariate normal, with distribution

$$d_1(\theta_1) = \mathcal{N}(x^*; A) \quad \text{where} \quad A = (\Sigma^{-1} + V^{-1})^{-1} \quad \text{and} \quad x = A(V^{-1}\hat{\theta}_1)$$

Here as above $\hat{\theta}_1$ and V are the effect size and covariance estimated in discovery data.

To assess the implications of choosing different value of ρ for inference, we compute the joint distribution of parameters given discovery data. This is

$$P(\theta_1, \theta_2|D_1) = \mathcal{M}\mathcal{V}\mathcal{N}(y; B)$$

where $B = \left(\begin{pmatrix} \Sigma & \rho\Sigma \\ \rho\Sigma & \Sigma \end{pmatrix}^{-1} + \begin{pmatrix} V^{-1} & 0 \\ 0 & 0 \end{pmatrix} \right)^{-1}$ and $y = B \cdot \begin{pmatrix} V^{-1}\hat{\theta}_1 \\ 0 \end{pmatrix}$. The matrix B can be solved using block inversion, giving

$$\begin{aligned} B &= \begin{pmatrix} \frac{1}{1-\rho^2}\Sigma^{-1} + V^{-1} & -\frac{\rho}{1-\rho^2}\Sigma^{-1} \\ -\frac{\rho}{1-\rho^2}\Sigma^{-1} & \frac{1}{1-\rho^2}\Sigma^{-1} \end{pmatrix}^{-1} \\ &= \begin{pmatrix} A & \rho A \\ \rho A & (1-\rho^2)\Sigma + \rho^2 A \end{pmatrix} \end{aligned}$$

Thus, the marginal distribution on the replication parameters θ_2 , given the discovery data D_1 , is

$$\theta_2|D_1 \sim \mathcal{M}\mathcal{V}\mathcal{N}(\rho A \cdot V^{-1}\hat{\theta}_1; (1-\rho^2)\Sigma + \rho^2 \cdot A)$$

Note that when $\rho = 0$ (no assumed correlation between discovery and replication effect sizes), this says that $\theta_2|D_1$ is distributed according to the prior effect size distribution, while when $\rho = 1$, $\theta_2|D_1$ reduces to the expression for $\theta_1|D_1$, as expected if these parameters are perfectly correlated. In the one-dimensional case, writing σ and v for the corresponding variances, the expression becomes

$$\theta_2|D_1 \sim \mathcal{N}\left(\frac{\rho\sigma\hat{\theta}_1}{v+\sigma}; (1-\rho^2)\sigma + \frac{\rho^2 v\sigma}{v+\sigma}\right)$$

Supplementary Figure 20 shows the distribution $\theta_2|D_1$ (y axis, solid and dashed lines) for a fixed observed discovery effect size, a range of values of the discovery standard error \sqrt{v} , and four choices of ρ . In the main replication analysis presented here we use $\rho = 0.9$.

Supplementary Note 6 - Genome-wide implementation of multinomial logistic regression

Introduction

We consider the problem of fitting a regression model for each of a large number of SNPs against a single categorical phenotype. The method described here is implemented in the software SNPTEST (see **Code Availability**).

Multinomial logistic regression for association testing

Let $\bar{Y} = (Y_i)_{i=1}^N$ denote a set of measurements of a categorical outcome variable on N samples. Each Y_i is assumed to take on one of $M + 1$ possible values labelled $0, 1, \dots, M$. Also, let $\bar{X} = (X_i)$ denote a set of measured covariates for each sample and $\bar{G} = (G_i)$ a predictor of interest. In the context of our study, Y_i is the severe malaria phenotype of sample i , with levels 0=Control, 1 = Cerebral malaria, 2 = Severe malarial anaemia, 3 = Other severe malaria, and G_i denotes the genotype of sample i at the variant under consideration.

Multinomial logistic regression models the log-odds of outcome level i , relative to the baseline level 0, as a linear combination of predictor and covariates. For a single sample this can be written as

$$\text{logodds}(Y = i | G = g, X = x, \theta) = z(g, x) \cdot \theta_i$$

or in terms of outcome probabilities as

$$P(Y = i | G = g, X = x, \theta) = \frac{e^{z(g, x) \cdot \theta_i}}{1 + \sum_{j=1}^J e^{z(g, x) \cdot \theta_j}} \quad (6)$$

where

1. $z(g, x)$ denotes the row vector $[1 \ g \ x]$, consisting of a single 1, the genotype g , and the row vector X of measured covariates. More generally we will write $z(g, x) = [1 \ F(g) \ x]$ where $F(g)$ is a function of the predictor used to model nonadditive effects, as described below.
2. θ_j denotes a column vector of parameters for outcome $j > 0$. (We always treat $j = 0$ as the baseline outcome, which in the above corresponds assuming that $\theta_0 \equiv 0$.)

The term $F(g)$ in our study is used to encode different models of effect, as follows. We assume variants are biallelic and let $a(g)$ and $b(g)$ be the counts of the first and second alleles carried by genotype g . The table below specifies how different common models of association are encoded in this scheme.

Model	Encoding
Additive	$F(g) = b(g)$
Dominant	$F(g) = \begin{cases} 1 & \text{if } b(g) > 0 \\ 0 & \text{otherwise} \end{cases}$
Recessive	$F(g) = \begin{cases} 1 & \text{if } b(g) = 2 \\ 0 & \text{otherwise} \end{cases}$
Heterozygote	$F(g) = \begin{cases} 1 & \text{if } b(g) = 1 \\ 0 & \text{otherwise} \end{cases}$
General	$F(g) = \begin{cases} \begin{bmatrix} 0 & 0 \end{bmatrix} & \text{if } b(g) = 0 \\ \begin{bmatrix} 1 & 1 \end{bmatrix} & \text{if } b(g) = 1 \\ \begin{bmatrix} 2 & 0 \end{bmatrix} & \text{if } b(g) = 2 \end{cases}$
Null model	$F(g)$ empty, i.e. no genotype predictor

Multinomial regression for directly-typed genotypes

For N samples, the full likelihood can be written as

$$\begin{aligned} P(\bar{Y} | \bar{G}, \bar{X}, \theta) &= \prod_{n=1}^N P(Y = Y_n | G = G_n, X_n, \theta) \\ &= \prod_n f(Y_n; G_n, X_n, \theta) \end{aligned}$$

up to a multiplicative constant, where

$$f(y; g, x, \theta) = \frac{e^{z(g,x) \cdot \theta_i}}{1 + \sum_{j=1}^J e^{z(g,x) \cdot \theta_j}} \quad (7)$$

The log-likelihood is then

$$\ell(\theta) = \log P(\bar{Y} | \bar{G}, \bar{X}, \theta) = \sum_{n=1}^N \log f(Y_n; G_n, X_n, \theta) \quad (8)$$

For each SNP, we first fit the null model iteratively starting from $\theta^{\text{null}} \equiv 0$. We then fit the full model starting from the parameters fit under the null model. We use Newton-Raphson iterations to fit both models. This requires computing the first and second derivatives of Supplementary Equation (8), as described below.

A key assumption underlying the product in Supplementary Equation (8) is that the outcome for each sample, given its covariates and genotype, is independent of all the other data, i.e.

$$P(Y = Y_n | \bar{Y}_{-n}, G, \bar{I}, \bar{X}, \theta) = f(Y_n; G_n, X_n, \theta) \quad (9)$$

For this to be reasonable in practice, this implies that the covariates X must capture relevant confounding effects, such as environmental effects on the phenotype that are shared between samples. In practice we use principal components computed from genome-wide genotypes as covariates, thus capturing geographic and population structure.

Multinomial regression for imputed genotypes

We now consider the case where the predictors are not directly observed but are probabilistically inferred from other, observed quantities. In the GWAS context this corresponds to the situation where genotypes at a variant are imputed from surrounding SNPs, giving a probability distribution over genotypes.

Write p for the function giving the distribution of genotypes at the untyped SNP across the N samples, given the other quantities,

$$p(g_1, \dots, g_N) = P(G = g_1, \dots, g_N | I, X, \theta, s)$$

Here I is used to denote the directly observed genotype data i.e. the genotypes at all directly typed SNPs. The symbol s denotes the fact of having been sampled in the study; we omit this from further notation but return to it below. The full likelihood can now be written by summing over the unobserved genotypes,

$$P(Y = \bar{Y} | I, X = \bar{X}, \theta) = \sum_{g_1, \dots, g_N} P(\bar{Y} | G = g_1, \dots, g_N, \bar{X}, \theta) p(g_1, \dots, g_N) \quad (10)$$

We make additional assumptions that make Supplementary Equation (10) tractible.

First, we assume that the genotypes at the chosen SNP for each sample are independent of all the genotypes and covariates of all other samples. Namely we write

$$p_n(g_n) = P(G_n = g | G_{-n} = g_1, \dots, g_N, I, X, \theta) = P(G_n = g | I_n, X_n, \theta) \quad (11)$$

This assumption lets us split the likelihood over samples

$$\begin{aligned} P(Y = \bar{Y} | I, X = \bar{X}, \theta) &= \sum_{g_1, \dots, g_N} P(\bar{Y} | G = g_1, \dots, g_N, \bar{X}, \theta) p(g_1, \dots, g_N) \\ &= \sum_{g_1, \dots, g_N} \prod_n f(Y_n; G_n, X_n, \theta) \cdot p_n(g_n) \\ &= \prod_n \sum_g f(Y_n; g, X_n, \theta) \cdot p_n(g) \end{aligned}$$

The last row holds because the n th term in the product does not involve g_m for any $m \neq n$, allowing us to reverse the order of the sum and product.

We make a further approximation by taking p_n as the probability distribution estimated by genotype imputation - i.e. using IMPUTE2 in our study. IMPUTE2 uses a reference panel of known haplotypes to infer genotypes based on surrounding typed SNPs. We note two ways in which this approximation may become inaccurate. First, if the reference panel populations and study populations are not well matched, i.e. if haplotypes are at substantially different frequencies in the panel and study, then imputation is likely to be inaccurate. (We address this in main text by incorporating population-specific haplotypes into our

reference panel.) Second, as described above, $p(g)$ is conditional on covariates, on the effect size parameter θ , and on the fact of having been sampled. IMPUTE2 does not take into account these factors. In particular, dropping covariates from the notation, and writing κ_j for the frequency of phenotype level j in the study and K_j for its frequency in the study population, we have

$$\begin{aligned} P(G = g|\theta, s) &= \sum_{j=0}^M P(G = g|Y = j, \theta) \cdot \kappa_j \\ &= \sum_{j=0}^M \frac{P(Y = j|G = g, \theta)P(G = g|\theta)}{P(Y = j|\theta)} \kappa_j \end{aligned} \quad (12)$$

$$= \left(\sum_{j=0}^M f(j; g, \theta) \cdot \frac{\kappa_j}{K_j} \right) \cdot \text{freq}(g) \quad (13)$$

Where $\text{freq}(g)$ is the frequency of genotype g in the study population. Thus if θ is substantially nonzero, then differences between study and population phenotype frequencies, e.g. due to upsampling of disease cases, lead to differences in genotype distributions that are not modelled by imputation. In practice we focus attention on well-imputed genotypes, and we expect most GWAS effect sizes to be small so that these inaccuracies are minor.

Derivatives of the complete data log-likelihood

To implement Newton-Raphson iterations for the model described above we need to compute the loglikelihood and its first and second derivatives. We first do this for the case when all genotypes are known (Supplementary Equation (8)) and then turn to the full model (Supplementary Equation (10)).

Write $f_j(\theta) = f(y; g, x, \theta)$, for given outcome level y , considered as a function of θ . We suppress g and x from the notation for a moment. Also we write $z = z(g, x)$ and D_j denotes the operation of taking the derivative with respect to the column vector θ_j . With this notation

$$f_i = \frac{e^{z\theta_i}}{1 + \sum_{j=1}^J e^{z\theta_j}}$$

By the quotient rule,

$$\begin{aligned} D_j f_i &= \frac{D_j e^{z\theta_i}}{1 + \sum_{l=1}^J e^{z\theta_l}} - \frac{e^{z\theta_i} \cdot D_j e^{z\theta_j}}{(1 + \sum_{l=1}^J e^{z\theta_l})^2} \\ &= z^t \cdot \begin{cases} f_i(1 - f_i) & \text{if } i = j \\ -f_i f_j & \text{if } i \neq j \end{cases} \\ &= z^t f_i (\psi_{i,j} - f_j) \quad \text{where} \quad \psi_{i,j} = \begin{cases} 1 & \text{if } j=i \\ 0 & \text{otherwise} \end{cases} \end{aligned} \quad (14)$$

since $D_j e^{z\theta_l} = 0$ if $l \neq j$. (Note that f_i are scalar-valued functions, so the result of each of these expressions is a row vector reflecting the derivative of f_i with respect to the entries of θ_j .)

Next we take second partial derivatives by applying the product rule to the expressions in Supplementary Equation (14):

$$\begin{aligned} D_k D_j f_i &= z \otimes z^t \cdot (D_k f_i (\psi_{ij} - f_j) - f_i \cdot D_k f_j) \\ &= z \otimes z^t \cdot f_i ((\psi_{i,j} - f_j)(\psi_{i,k} - f_k) - f_j(\psi_{j,k} - f_k)) \end{aligned} \quad (15)$$

Here $z \otimes z^t$ denotes the Kronecker product (i.e. the matrix of all pairwise multiples of elements of z).

The above expressions show that, even though each individual has single assigned outcome, it is useful to compute f_i over all possible outcome levels, since these values can be reused when computing the derivatives.

Remark: the log-likelihood and derivatives are now given by

$$\ell = \sum_n \log f(Y_n; G_n, X_n, \theta) = \sum_n \log f \quad (16)$$

$$D\ell = \sum_n \frac{Df}{f} \quad (17)$$

$$D^2\ell = \sum_n \left(\frac{D^2f}{f} - \frac{Df^{\otimes 2}}{f^2} \right) \quad (18)$$

The derivative over all parameters can be computed blockwise for given outcome levels using Supplementary Equations (14) and (15).

Derivatives of the full log-likelihood

Now consider the full likelihood (Supplementary Equation (10)), i.e. the likelihood allowing for imputed predictor variables. The log-likelihood is

$$\ell^{\text{full}}(\theta) = \sum_n h_n \quad \text{where} \quad h_n = \log \sum_g f(Y_n; g, X_n, \theta) \cdot p_n(g)$$

Consider one term of the outer sum, say the n -th term $h = h_n$. Similar to what we did before, write $f_{i,g}(\theta) = f(i; g, X_n, \theta)$ where i is an outcome level. Then

$$h = \log \sum_g f_{Y_n,g} \cdot p_n(g)$$

$$D_j h = \frac{\sum_g D_j f_{Y_n,g} \cdot p_n(g)}{\sum_g f_{Y_n,g} \cdot p_n(g)} \quad (19)$$

(Here we have used the simplifying assumption that $p_n(g)$, computed from imputation, does not depend on θ , and hence does not affect the derivative).

The second derivative is

$$D_k D_j h = D_k \left(\frac{\sum_g D_j f_{Y_n,g} \cdot p_n(g)}{\sum_g f_{Y_n,g} \cdot p_n(g)} \right)$$

$$= \frac{\sum_g D_k D_j f_{Y_n,g} \cdot p_n(g)}{\sum_g f_{Y_n,g} \cdot p_n(g)} - \frac{(\sum_g D_j f_{Y_n,g} \cdot p_n(g)) \otimes (\sum_g D_k f_{Y_n,g} \cdot p_n(g))}{(\sum_g f_{Y_n,g} \cdot p_n(g))^2}$$

$$= \left(\frac{\sum_g D_k D_j f_{Y_n,g} \cdot p_n(g)}{\sum_g f_{Y_n,g} \cdot p_n(g)} \right) - (D_j h \otimes D_k h) \quad (20)$$

Implementation

In our implementation, we rely on a linear algebra library (Eigen) which deals with vectors and matrices. To simplify this we first collect the parameters in a single column vector, as

$$\theta = [\theta'_1 \quad \theta'_2 \quad \dots \quad \theta'_M]^t$$

With this convention, $D\ell$ becomes a $1 \times dM$ row vector, and the second derivative $D^2\ell$ is represented as a $dM \times dM$ matrix.

The expressions for the loglikelihood and its derivatives share common terms. We take advantage of these to reduce computation. Define coefficients A, B, C as

$$A_{n,g} = \frac{f_{Y_n,g} \cdot p_n(g)}{\sum_h f_{Y_n,h} \cdot p_n(h)}$$

and

$$B_{n,g,j} = A_{n,g} \cdot (\psi_{Y_n,j} - f_{j,g})$$

and

$$C_{n,g,j,k} = A_{n,g} \cdot ((\psi_{Y_n,k} - f_{k,g})(\psi_{Y_n,j} - f_{j,g}) - f_{j,g}(\psi_{j,k} - f_{k,g}))$$

Then by the above:

$$D_j \ell = \sum_g \sum_n (z_n(g)^t \cdot B_{n,g,j}) = \sum_g \text{diag}(B_{\cdot,g,j}) \times Z(g) \quad (21)$$

where $\text{diag}(B_{\cdot,g,j})$ denotes the diagonal matrix with n th diagonal entry equal to $B_{n,g,j}$. This can be implemented by matrix multiplication. Similarly

$$D_k D_j \ell = \sum_g \sum_n (z_n(g) \otimes z_n(g)^t \cdot C_{n,g,j,k}) - \sum_n ((D_j \ell)^t \otimes (D_k \ell)) \quad (22)$$

We follow this implementation strategy, first computing $f_{i,g}$ for each sample and outcome level, using this to compute the loglikelihood and $A_{n,g}$. We then compute $B_{n,g,j}$ and $C_{n,g,j,k}$ and use these to compute the first and second derivative.

Supplementary Note 7 - Multidimensional inverse variance-weighted meta-analysis

Let $\hat{\beta}_i$ be a parameter estimate from logistic regression in population i , and let V_i denote the estimated variance-covariance matrix of $\hat{\beta}_i$. We compute the meta-analysis estimate $\hat{\beta}_{\text{meta}}$ as

$$V_{\text{meta}} = \left(\sum_i V_i^{-1} \right)^{-1} \quad \text{and} \quad \hat{\beta}_{\text{meta}} = V_{\text{meta}} \cdot \left(\sum_i V_i^{-1} \hat{\beta}_i \right) \quad (23)$$

We note that $\hat{\beta}_{\text{meta}}$ is also equal to the combined maximum likelihood estimate, under the assumption that the likelihood function in each population is gaussian with the given mean $\hat{\beta}_i$ and covariance V_i and all studies are independent. In the one-dimensional case, writing lower-case letters for the scalar quantities instead of matrices, Supplementary Equation (23) reduces to

$$v_{\text{meta}} = \frac{1}{\sum_i \frac{1}{v_i}} \quad \text{and} \quad \hat{\beta}_{\text{meta}} = v_{\text{meta}} \cdot \sum_i \frac{1}{v_i} \hat{\beta}_i$$

A two-tailed p-value for β can thus be computed by performing a Wald test, comparing $\hat{\beta}_{\text{meta}}$ to the normal distribution with mean 0 and variance v_{meta} .

In the general case, suppose $\hat{\beta}$ is d -dimensional (e.g. representing effects on d subphenotypes). A p-value for each component of $\hat{\beta}_{\text{meta}}$ can be obtained by a Wald test using the corresponding diagonal entry of V_{meta} . To obtain a global p-value against the null that all parameters are zero, let $V_{\text{meta}} = LL^t$ be the Cholesky decomposition of V_{meta} and $a = L^{-1} \hat{\beta}_{\text{meta}}$. Then

$$\text{var}(a) = \text{Id}$$

We can therefore compute a p-value by computing the sum of squared entries,

$$\zeta = \sum_{k=1}^d a_k^2 \quad \text{such that} \quad \zeta \sim \chi_d^2$$

and computing a p-value from quantiles of the χ^2 distribution.

In the interpretation of p-values as the probability of obtaining an estimate “as extreme, or more extreme” than the observed estimate, under the null model, we note that this treats points as “more extreme” when they have lower probability in the full likelihood $\mathcal{N}(0; V_{\text{meta}})$.

In practice the Cholesky decomposition does not need to be computed directly, because

$$\begin{aligned} \zeta &= a^t a = \hat{\beta}_{\text{meta}}^t L^{t-1} L^{-1} \hat{\beta}_{\text{meta}} \\ &= \left(\sum_i V_i^{-1} \hat{\beta}_i \right)^t V_{\text{meta}} \cdot V_{\text{meta}}^{-1} \cdot V_{\text{meta}} \left(\sum_i V_i^{-1} \hat{\beta}_i \right)^t \\ &= \left(\sum_i V_i^{-1} \hat{\beta}_i \right) \cdot \hat{\beta}_{\text{meta}} \end{aligned}$$

Thus, the terms of the sum can be computed from $\hat{\beta}_{\text{meta}}$ and the left hand term, which is already computed as part of Supplementary Equation (23).

Supplementary Note 8 - Analysis of population differentiation

Main text presents an analysis of allele frequency differentiation between continents and between African populations for associated variants (**Fig 7a**). We note here further details of this analysis.

Our between-continent analysis highlights an essential difficulty in making between-continent comparisons of this type for individual variants, namely that it is difficult for protective alleles below around 20-30% frequency to achieve extreme ranks. This is true even for strong resistance alleles that are essentially only present in Africa (e.g. HbS, $\text{rank}_{\text{EUR|AFR}} = 0.18$; DUP4, $\text{rank}_{\text{EUR|AFR}} = 0.44$), and presumably reflects the fact that a large number of low-frequency alleles were lost during ancestral bottlenecks in the history of non-African populations. This suggests that, while the observation of elevated frequencies in Africa for particular mutations might imply the action of selection due to *P.falciparum* malaria, as is frequently suggested^{18,37,38}, it might be equally consistent with neutral evolution under the high levels of genetic drift experienced by historical populations.

In main text we noted enrichment for high levels of within-Africa differentiation among variants with the highest evidence for association (Main text and figure **7b-c**). We note here specific alleles with evidence for differentiation. Most prominent among these is the glycoporin variant DUP4 ($P_{X|X} = 1.8 \times 10^{-5}$), which as reported previously⁷ is only present at high frequency in east African populations (maximum observed frequency = 0.2% in populations west of Cameroon; frequency = 3.8%, 4.5% and 9.0% in Malawi, Tanzania and Kenya respectively). Another associated variant, rs56292300 in *AP2BI*, is of interest since it appears differentiated both within Africa and between continents ($BF_{\text{avg}} = 4,511$; $P_{X|X} = 4 \times 10^{-3}$ $\text{rank}_{\text{EUR|AFR}} = 0.035$). This reflects the fact that the protective allele, which also appears to be ancestral, is at much lower frequency in European and Asian populations (84-88%) than in Africa (~98%). Notably, however, rs56292300 is one of a number of variants that show considerable heterogeneity both in frequency and in estimated effect size across populations (e.g. identified as those with maximum Bayes factor ($BF_{\text{max}} > 25,000$ and 100 times greater than the fixed-effect Bayes factor; **Supplementary Data 1**). The possibility of geographically localized effects, or for locus-specific confounding driven by gradients in selection pressure, cannot be discounted. Fully unraveling such signals is likely to require amalgating data at finer geographic scales^{22,39}.

Supplementary References

1. Malaria Genomic Epidemiology, N., Band, G., Rockett, K.A., Spencer, C.C. & Kwiatkowski, D.P. A novel locus of resistance to severe malaria in a region of ancient balancing selection. *Nature* **526**, 253-7 (2015).
2. MalariaGEN. Reappraisal of known malaria resistance loci in a large multi-centre study. *Nature Genetics* (2014).
3. Shah, S.S. *et al.* Heterogeneous alleles comprising G6PD deficiency trait in West Africa exert contrasting effects on two major clinical presentations of severe malaria. *Malar J* **15**, 13 (2016).
4. Clarke, G.M. *et al.* Characterisation of the opposing effects of G6PD deficiency on cerebral malaria and severe malarial anaemia. *Elife* **6**(2017).
5. Jallow, M. *et al.* Genome-wide and fine-resolution association analysis of malaria in West Africa. *Nat Genet* **41**, 657-65 (2009).
6. Band, G. *et al.* Imputation-based meta-analysis of severe malaria in three African populations. *PLoS Genet* **9**, e1003509 (2013).
7. Leffler, E.M. *et al.* Resistance to malaria through structural variation of red blood cell invasion receptors. *Science* **356**(2017).
8. Busby, G.B. *et al.* Admixture into and within sub-Saharan Africa. *Elife* **5**(2016).
9. Toure, O. *et al.* Candidate polymorphisms and severe malaria in a Malian population. *PLoS One* **7**, e43987 (2012).
10. Olaniyan, S.A. *et al.* Tumour necrosis factor alpha promoter polymorphism, TNF-238 is associated with severe clinical outcome of falciparum malaria in Ibadan southwest Nigeria. *Acta Trop* **161**, 62-7 (2016).
11. Apinjoh, T.O. *et al.* Association of cytokine and Toll-like receptor gene polymorphisms with severe malaria in three regions of Cameroon. *PLoS One* **8**, e81071 (2013).
12. Apinjoh, T.O. *et al.* Association of candidate gene polymorphisms and TGF-beta/IL-10 levels with malaria in three regions of Cameroon: a case-control study. *Malar J* **13**, 236 (2014).
13. Manjurano, A. *et al.* Candidate human genetic polymorphisms and severe malaria in a Tanzanian population. *PLoS One* **7**, e47463 (2012).
14. Manjurano, A. *et al.* USP38, FREM3, SDC1, DDC, and LOC727982 Gene Polymorphisms and Differential Susceptibility to Severe Malaria in Tanzania. *J Infect Dis* (2015).
15. Manjurano, A. *et al.* African glucose-6-phosphate dehydrogenase alleles associated with protection from severe malaria in heterozygous females in Tanzania. *PLoS Genet* **11**, e1004960 (2015).
16. Sepulveda, N. *et al.* Malaria Host Candidate Genes Validated by Association With Current, Recent, and Historical Measures of Transmission Intensity. *J Infect Dis* **216**, 45-54 (2017).
17. Ravenhall, M. *et al.* Novel genetic polymorphisms associated with severe malaria and under selective pressure in North-eastern Tanzania. *PLoS Genet* **14**, e1007172 (2018).
18. Opi, D.H. *et al.* Two complement receptor one alleles have opposing associations with cerebral malaria and interact with alpha(+)thalassaemia. *Elife* **7**(2018).
19. Ndila, C.M. *et al.* Human candidate gene polymorphisms and risk of severe malaria in children in Kilifi, Kenya: a case-control association study. *Lancet Haematol* **5**, e333-e345 (2018).
20. Shah, S.S. *et al.* Genetic determinants of glucose-6-phosphate dehydrogenase activity in Kenya. *BMC Med Genet* **15**, 93 (2014).
21. Uyoga, S. *et al.* Glucose-6-phosphate dehydrogenase deficiency and the risk of malaria and other diseases in children in Kenya: a case-control and a cohort study. *Lancet Haematol* **2**, e437-44 (2015).
22. Mackinnon, M.J. *et al.* Environmental Correlation Analysis for Genes Associated with Protection against Malaria. *Mol Biol Evol* **33**, 1188-204 (2016).
23. Kariuki, S.M. *et al.* The genetic risk of acute seizures in African children with falciparum malaria. *Epilepsia* **54**, 990-1001 (2013).

24. Muriuki, J.M. *et al.* The ferroportin Q248H mutation protects from anemia, but not malaria or bacteremia. *Sci Adv* **5**, eaaw0109 (2019).
25. Dunstan, S.J. *et al.* Variation in human genes encoding adhesion and proinflammatory molecules are associated with severe malaria in the Vietnamese. *Genes Immun* **13**, 503-8 (2012).
26. Manning, L. *et al.* A Toll-like receptor-1 variant and its characteristic cellular phenotype is associated with severe malaria in Papua New Guinean children. *Genes Immun* **17**, 52-9 (2016).
27. Flint, J., Harding, R.M., Boyce, A.J. & Clegg, J.B. The population genetics of the haemoglobinopathies. *Baillieres Clin Haematol* **11**, 1-51 (1998).
28. Higgs, D.R. The molecular basis of alpha-thalassemia. *Cold Spring Harb Perspect Med* **3**, a011718 (2013).
29. Williams, T.N. & Weatherall, D.J. World distribution, population genetics, and health burden of the hemoglobinopathies. *Cold Spring Harb Perspect Med* **2**, a011692 (2012).
30. Lam, K.W. & Jeffreys, A.J. Processes of copy-number change in human DNA: the dynamics of {alpha}-globin gene deletion. *Proc Natl Acad Sci U S A* **103**, 8921-7 (2006).
31. Crosnier, C. *et al.* Basigin is a receptor essential for erythrocyte invasion by Plasmodium falciparum. *Nature* **480**, 534-7 (2011).
32. Wellcome Trust Case Control, C. *et al.* Bayesian refinement of association signals for 14 loci in 3 common diseases. *Nat Genet* **44**, 1294-301 (2012).
33. McLaren, W. *et al.* The Ensembl Variant Effect Predictor. *Genome Biol* **17**, 122 (2016).
34. Alvarez, M.I. *et al.* Human genetic variation in VAC14 regulates Salmonella invasion and typhoid fever through modulation of cholesterol. *Proc Natl Acad Sci U S A* **114**, E7746-E7755 (2017).
35. Dunstan, S.J. *et al.* Variation at HLA-DRB1 is associated with resistance to enteric fever. *Nat Genet* **46**, 1333-6 (2014).
36. Gilchrist, J.J. *et al.* Genetic variation in VAC14 is associated with bacteremia secondary to diverse pathogens in African children. *Proc Natl Acad Sci U S A* **115**, E3601-E3603 (2018).
37. Ma, S. *et al.* Common PIEZO1 Allele in African Populations Causes RBC Dehydration and Attenuates Plasmodium Infection. *Cell* **173**, 443-455 e12 (2018).
38. Zhang, D.L. *et al.* Erythrocytic ferroportin reduces intracellular iron accumulation, hemolysis, and malaria risk. *Science* **359**, 1520-1523 (2018).
39. Piel, F.B. *et al.* Global distribution of the sickle cell gene and geographical confirmation of the malaria hypothesis. *Nat Commun* **1**, 104 (2010).